Russian Chemical Reviews **85** (3) 280 – 307 (2016)

DOI 10.1070/RCR4554

Metal-organic frameworks: structure, properties, methods of synthesis and characterization

V V Butova,[a] M A Soldatov,[a] A A Guda,[a] K A Lomachenko,[a, b] C Lamberti [a, b]

[a] International Research Center 'Smart Materials', Southern Federal University
ul. Zorge 5, Rostov-on-Don, 344090 Russian Federation
[b] Department of Chemistry, NIS and CrisDi Interdepartmental Centers, INSTM Reference Center, University of Turin
Via P Giuria 7, I-10125 Turin, Italy

This review deals with key methods of synthesis and characterization of metal-organic frameworks (MOFs). The modular structure affords a wide variety of MOFs with different active metal sites and organic linkers. These compounds represent a new stage of development of porous materials in which the pore size and the active site structure can be modified within wide limits. The set of experimental methods considered in this review is sufficient for studying the short-range and long-range order of the MOF crystal structure, determining the morphology of samples and elucidating the processes that occur at the active metal site in the course of chemical reactions. The interest in metal-organic frameworks results, first of all, from their numerous possible applications, ranging from gas separation and storage to chemical reactions within the pores.
The bibliography includes 362 references.

Contents

I. Introduction

Metal-organic frameworks (MOFs) represent a new class of porous materials. They have a modular structure, which offers enormous structural diversity and wide possibilities for creation of materials with tailored properties. MOFs are produced by different methods, both traditional and rather specific ones, with the use of microwave, ultrasonic, mechanochemical and electrochemical processing. Here, of crucial importance is the reproducibility of the results of synthesis and postsynthetic treatment of the produced samples. MOFs are frequently additionally functionalized to make them suitable for specific application.

In recent decades, the possibility to vary the structure porosity, topology and elemental composition (the Al : Si ratio and isomorphous substitution of transition metal atoms in tetrahedral positions) has rendered zeolites [1, 2] and their derivatives [3 – 7] the most appropriate materials for

V V Butova Researcher at the International Research Center 'Smart Materials' at the SFedU. E-mail: ButovaV86@gmail.com
Current research interests: metal-organic frameworks, zeolites, solid ionic electrolytes.
M A Soldatov PhD in Physics and Mathematics, Leading Researcher at the same Center. E-mail: mikhail.soldatov@gmail.com
A A Guda PhD in Physics and Mathematics, Leading Researcher at the same Center. E-mail: guda@sfedu.ru
Current research interests of the authors: X-ray absorption spectroscopy, materials science.

K A Lomachenko Junior Researcher at the same Center, PhD Student at the University of Turin. E-mail: kirlom@gmail.com
Current research interests: materials science, synchrotron radiation, catalysis.
C Lamberti Professor, Department of Chemistry, NIS and CrisDi Interdepartmental Centers, INSTM Reference Center, University of Turin. Telephone: +39(011)670 – 7841, e-mail: carlo.lamberti@unito.it
Current research interests: zeolites, metal-organic frameworks, metal nanoparticles, semiconductors, superconductive materials.

Received 30 December 2014
Uspekhi Khimii **85** (3) 280 – 307 (2016); translated by G A Kirakosyan

use in a variety of fields: in gas adsorption [8,9] and separation [10,11], catalysis,[12–16] photocatalysis,[17–19] and in design of materials in which the quantum properties of encapsulated phases are used;[20–23] these applications have been covered in reviews.[24,25] Zeolites and their derivatives have been addressed in experimental [26–29] and theoretical [30–34] studies.

However, MOFs are superior to zeolites in many respects;[6,35–51] in particular, a distinctive feature of MOFs is the large surface area. The MOF consists of secondary building units connected by organic linkers. These secondary building units are metal ions or clusters coordinated by oxygen or nitrogen atoms, and much more rarely by fluorine and other nonmetal atoms.[52]

Metal-organic frameworks differ from zeolites in many important aspects.[53,54] The key difference of the MOFs is a wide diversity and variability of their structure in combination with lower topological restrictions on the formation of porous three-dimensional frameworks. A significant number of new MOF structures synthesized every year confirms this variability and heightened interest in their potential application areas.[55] Zeolites are built of tetrahedral fragments, and differences in their topology are based on a finite number of secondary structure elements,[56] whereas inorganic secondary building units of MOFs can be both a separate metal atom or a more or less complicated cluster and one-, two- or three-dimensional extended inorganic substructures.

A combination of organic and inorganic structure elements can lead to materials with unique properties. On the one hand, MOFs are characterized by high strength and considerable pore volume (50% of the total volume or more). On the other hand, the choice of the initial building units makes it possible to vary some parameters, such as the pore size (to increase pore diameter to 98 Å),[57] density (to decrease to 0.126 g cm^{-3}),[58] as well as the specific surface area (up to 1000–10 000 m^2 g^{-1}),[46] which opens up new ways to produce materials with tailored physicochemical properties.

Owing to their porous structure, larger specific surface area, stability and ability to be functionalized, MOFs are good candidates for use in gas separation, catalysis and ion exchange reactions where zeolites are traditionally used. By now, MOFs have essentially surpassed zeolites in pore size and pore specific volume; therefore, they can be used as selective catalysts in different reactions, including reactions with bulky molecules that cannot penetrate zeolite pores. Nevertheless, because of their structural features, MOFs still rank below zeolites in thermal stability. Although there are only a few examples of commercial use of MOFs,[59,60] it is predicted that in the near future, this class of materials will play an important role in very various fields:

— for gas separation and purification [61–65] (for example, for selective H_2 adsorption,[66] separation of CO_2 under near-normal conditions for biogas enrichment,[67–70] selective adsorption of CO_2 (Refs 71–73) and CH_4,[73] hydrocarbon separation,[74] selective adsorption of O_2,[75] air purification from toxic contaminants,[76,77] enantioselective sorption of alcohols,[78] selective separation of a mixture of cyclo-S_4N_4 and benzene mixture [79] as stationary phases for gas chromatography [80]);

— for separation of liquid phases,[64,81–86] for adsorption and storage of different gases [87–91] and liquids (including H_2,[92–104] CH_4,[105–107] CO_2,[108–111] MeOH,[112] H_2S,[113,114] H_2O [115]);

— for creation of materials for heat pumps and absorption refrigerators,[115] materials for absorption and neutralization of toxic gases and fumes;[76]

— for targeted drug delivery;[116–119]

— for the development of optical and luminescent materials,[120–132] photoactive [133] and magnetic materials,[134–138] solid-state ionic [139,140] and proton conductors,[115,141–143] semiconductors,[144] materials for electronic and optoelectronic devices,[145] sensors;[62,132,145,146]

— for the development of different catalysts,[147–155] including those for enantioselective chiral reactions,[156–166] asymmetric epoxidation of alkenes [167] and allyl alcohols,[168] opening of epoxides with methanol,[169] benzaldehyde activation,[170] oxidation of alcohols,[171–174] allyl oxidation of cyclohexene,[175] the Suzuki [171] and Sonogashira reactions,[176,177] cross aldol condensation,[178] the Knoevenagel condensation,[179–181] alkene hydrogenation,[171] 'click' chemistry reactions,[182,183] cyanosilylation of organic carbonyl-containing substrates,[184] the Michael reaction and transesterification,[185] resynthesis of fat,[186] synthesis of cyclic carbonates from epoxides and CO_2,[187] acetalization of aldehydes with methanol;[188]

— in photocatalysis;[189,190]

— in synthesis of porous carbon materials through thermal decomposition of guest-free MOFs;[191]

— for synthesis of compounds in which the quantum properties of encapsulated phases are used.[192,193]

Studies dealing with the synthesis of stable MOFs with a high specific volume of internal pores, exactly specified pore size and periodic structure were initiated in the 1990s [194–196] and were inspired by the development of the idea of modular synthesis. The importance of these investigations was reflected in the special issue of *Microporous and Mesoporous Materials*, dedicated to synthesis, analysis of properties and application of MOFs.[197] The issue contained both reviews [198–201] and original papers.[170,202–207] The large amount of available experimental data on MOFs provided the basis for summarizing basic and applied results in detailed reviews (see, for example, Refs 89, 201, 208–219) and monographs.[220–222]

A key distinction of the present review is that it focuses simultaneously on the synthesis and analysis of metal-organic frameworks. Major attention is paid to specific features caused by the unique structure of this class of compounds. In particular, among the methods of analysis, X-ray absorption spectroscopy is of special importance since it serves to study the local environment of metal clusters surrounded by guest molecules, which is essential for the understanding of the MOF activity.

II. Nomenclature of metal-organic frameworks

In recent times, numerous materials containing metal ions bound by organic linkers have been described. These compounds have been differently named: metal-organic frameworks,[195] coordination polymers,[223–225] metal-organic polymers,[226] hybrid organic-inorganic materials [227] and organic zeolite analogues.[228] Attempts have been made to systematize and interpret the definitions used in this field.[53,201,229] Coordination polymer is among the most general terms denoting the existence of metal atoms (ions)

coordinated to ligands (in particular, through donor–acceptor bonds), but it does not specify the structure or morphology of a compound.[201] Noteworthy is the term porous structures, or open structures (frameworks), which implies that disordered unbound solvent molecules can pass through cavities of a definite structure (framework) and easily leave it. The term MOF implies not only the existence of a porous structure but also strong bonds responsible for the rigidity of a framework with a well-defined geometry in which connecting structural units can be replaced in the course of synthesis.[201] In other words, these objects should have a clearly pronounced crystal structure, which is a key criterion for establishing clear structure–property relationships.

Abbreviation MOF is usually used as a general name of the class of compounds; however, when followed by an ordinal number, it denotes an individual metal-organic framework (Table 1, lines 1–5). Analysis of a large number of structures and MOF properties made it possible to formulate criteria[230] for design of framework structures with desired properties as, for example, in the family of MOFs with the same symmetry IRMOF-1–IRMOF-16 (isoreticular metal-organic frameworks)[105] (see Table 1, lines 6, 7). Russian[231–234] and Chinese[235, 236] researchers often use the name 'metal-organic coordination polymers' with specified composition. Many MOFs are combined into classes with the same letter designation not according to the similarity of their structure (as in the above examples) but according to the place of their discovery. Such classes are, for example, UiO, MIL, HKUST, LIC, *etc.* (see Table 1, lines 8–19). Another large family of MOFs has the zeolite topology. Metal ions (Fe, Co, Cu, Zn, *etc.*) are surrounded by tetrahedra made of nitrogen atoms and are connected through imidazole rings, which can have different functionalities. Such MOFs are designated by the abbreviation ZIF (zeolite imidazolate framework) with a number (see Table 1, lines 20, 21). There are numerous designations corresponding to the classification of the research groups that synthesized these MOFs, for example, CPL, F-MOF-1, and MOP-1 (see Table 1, lines 22–24), *etc.*

As distinct from organic polymers for which the operational, physical and optical characteristics are, first of all, determined by the properties and the number of monomeric units in the chain, the properties of metal-organic frameworks are largely determined by the connectivity of building blocks in the framework.[230] Thus, synthesis of MOFs implies not only the choice of building units of the framework but also their specific organization in the solid phase.

Table 1. Examples of typical MOF names and their composition.

No.	Designation	Formula	Abbreviation interpretation
1	MOF-74	Zn_2DOT	Metal-Organic Frameworks
2	MOF-101	$Cu_2(BDC\text{-}Br)_2(H_2O)_2$	
3	MOF-177	$Zn_4O(BTB)_2$	
4	MOF-235	$[Fe_3O(BDC)_3(DMF)_3][FeCl_4]\cdot(DMF)_3$	
5	MOF-253	$Al(OH)(BPYDC)$	
6	IRMOF-1 (MOF-5)	$Zn_4O(BDC)_3\cdot 7\,DEF\cdot 3\,H_2O$	IsoReticular Metal-Organic Frameworks
7	IRMOF-16	$Zn_4O(TPDC)_3\cdot 17\,DEF\cdot 2\,H_2O$	
8	UiO-66	$Zr_6O_6(BDC)_6$	Universitetet i Oslo
9	UiO-67	$Zr_6O_6(BPDC)_6$	
10	UiO-68	$Zr_6O_6(TPDC)_6$	
11	MIL-53	$Al(OH)(BDC)$	Materials of Institut Lavoisier
12	MIL-53(Al)-NH_2	$Al(OH)(BDC\text{-}NH_2)$	
13	MIL-88A	$Fe_3O(MeOH)_3(O_2CCH{=}CHCO_2)_3\cdot MeCO_2\cdot n\,H_2O$	
14	MIL-88-Fe	$Fe_3O(MeOH)_3(O_2C(CH_2)_2CO_2)_3\cdot AcO\cdot(MeOH)_{4.5}$	
15	MIL-88B-4CH_3	$2\,Fe_3O(OH)(H_2O)_2(BDC\text{-}Me_2)_3$	
16	MIL-100-Fe	$Fe^{III}_3O(H_2O)_2F\cdot(BTC)_2\cdot n\,H_2O$	
17	MIL-101	$Cr_3O(H_2O)_2F\cdot(BDC)_3\cdot n\,H_2O$	
18	HKUST-1 (MOF-199)	$Cu_3(BTC)_2$	Hong Kong University of Science and Technology
19	LIC-1	$Gd_2(BDC\text{-}NH_2)_3(DMF)_4$	Leiden Institute of Chemistry
20	ZIF-8	$Zn(MIM)_2$	Zeolite Imidazolate Framework
21	ZIF-90	$Zn(FIM)_2$	
22	CPL-2	$Cu_2(PZDC)_2(4,4'\text{-}BPY)$	Coordination Polymer with pillared Layer structure
23	F-MOF-1	$[Cu(HFBBA)(phen)_2](H_2HFBBA)_2(H_2O)(HCO_2)$	Fluorinated Metal-Organic Framework
24	MOP-1	$Cu_{24}(m\text{-}BDC)_{24}(DMF)_{14}(H_2O)_{10}$	Metal-Organic Polyhedra

Note. DOT is 2,5-dihydroxyterephthalate, BPYDC is 2,2′-bipyridine-5,5′-dicarboxylate, DEF is *N*,*N*-diethylformamide, TPDC is *p*-terphenyl-4,4′-dicarboxylate, BPDC is biphenyl-4,4′-dicarboxylate, MIM is 2-methylimidazolate, FIM is 2-formylimidazolate, PZDC is pyrazine-2,3-dicarboxylate, 4,4′-BPY is 4,4′-bipyridine, phen is 1,10-phenanthroline, HFBBA is 4,4′-(hexafluoroisopropylidene)dibenzoate, m-BDC is *m*-benzenedicarboxylate (for BDC, BDC-Br, BDC-NH_2, BDC-Me_2, BTB, BTC, see Fig. 1).

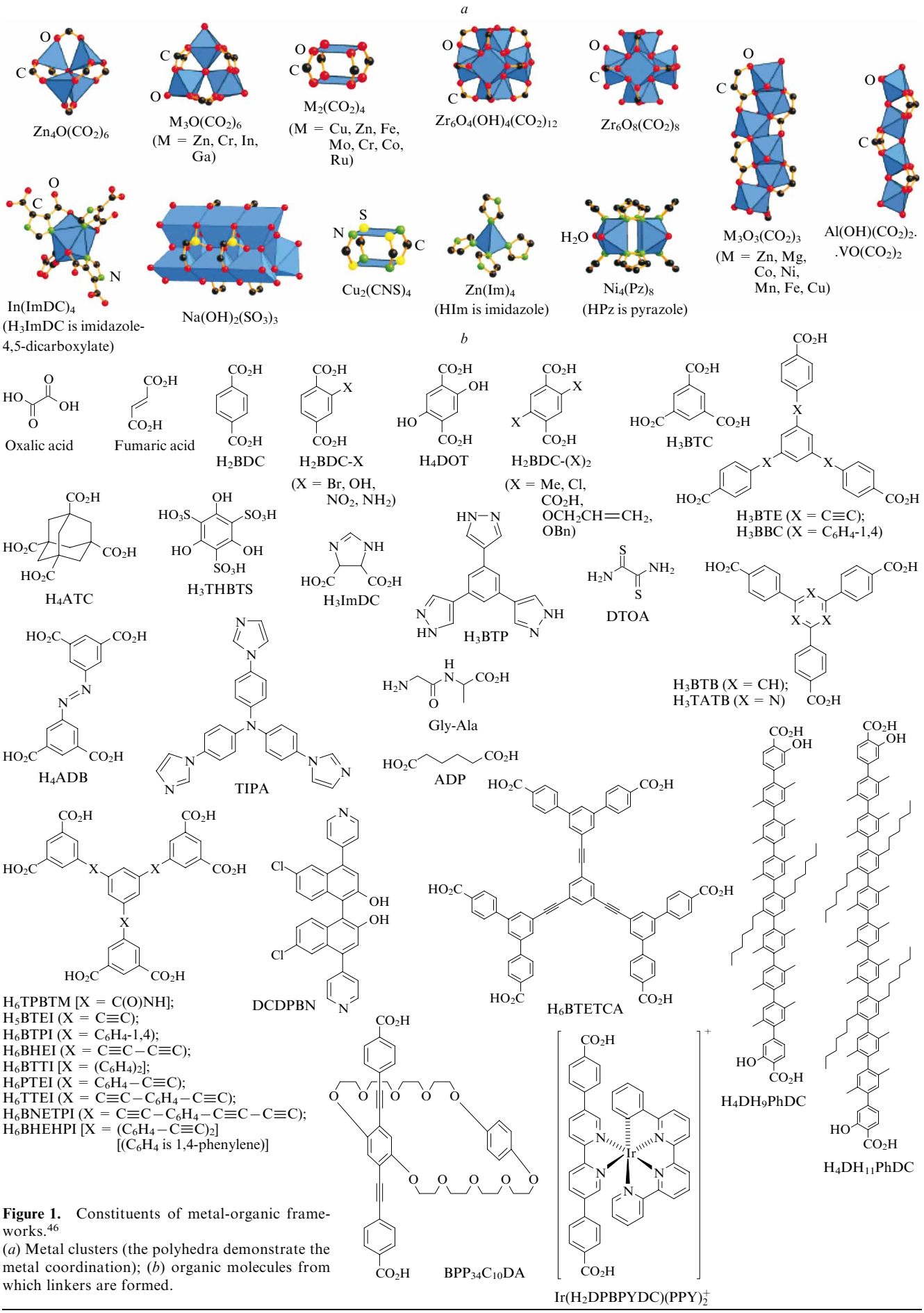

Figure 1. Constituents of metal-organic frameworks.[46]
(*a*) Metal clusters (the polyhedra demonstrate the metal coordination); (*b*) organic molecules from which linkers are formed.

III. Structural features of metal-organic frameworks

Two components can be distinguished in MOFs: secondary building units (Fig. 1 *a*) (clusters or metal ions) and organic molecules (Fig. 1 *b*) linking the former to give basically periodic porous structures. Different combinations of these structure elements lead to an enormous number of MOFs. In particular, 131 variants of the geometry of secondary building units had been deposited with the Cambridge Crystallographic Data Centre by 2007.[237]

In addition, in each geometry variant, the central metal atom can be substituted. In particular, the substitution of secondary building units, while the linker is the same — terephthalic acid, can lead to quite different MOFs (Fig. 2).

One of the first synthesized MOFs — MOF-5 — consists of tetrahedral ZnO_4 moieties located at the sites of a cubic lattice and connected with each other by linkers — terephthalate dianions. Elongating the carbon chain of the linker, the initial topology being retained, makes it possible to synthesize materials that have similar structure and symmetry but differ in pore size. The members of such a structural series are, as a rule, denoted with the code IRMOF followed by a number.

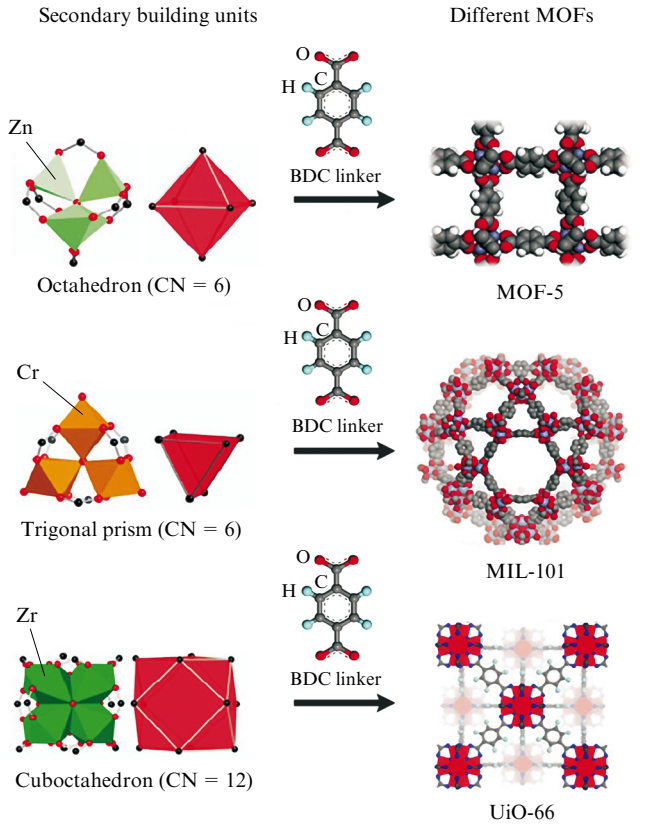

Figure 2. Structures of different MOFs with the terephthalate (BDC) dianion as a linker.[150]
The left panel shows oxygen coordination polyhedra around metal atoms in secondary building units, as well as the general shape of core clusters dictated by the arrangement of carbon atoms. The specified coordination numbers (CNs) correspond to the number of linkers coordinated to each cluster.

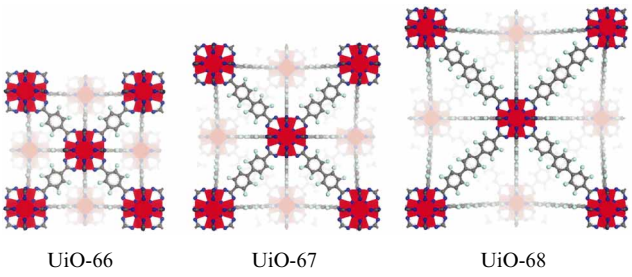

Figure 3. Framework symmetry retention with an increase in the linker chain length.[238]
The linker is terephthalate dianion in UiO-66, biphenyl-4,4′-dicarboxylate dianion in UiO-67 and terphenyl-4,4′-dicarboxylate dianion in UiO-68.

According to the classification proposed by Tranchemontagne *et al.*,[237] the coordination number of secondary building units can vary from 3 to 66.

Secondary building unites can be combined into a framework structure through different linkers. Selection and substitution of a linker can lead to two situations: either the symmetry of the structure is retained when another linker is used and only the unit cell parameters change because of the elongation of the carbon chain (for example, when going from UiO-66 to UiO-68) (Fig. 3) [103, 238, 239] or the symmetry can also change because of the change in the mutual arrangement of functionalities (Fig. 4).

As already mentioned, MOFs are distinguished by the diversity of their structure, different symmetry and pore sizes and, hence, by their characteristics. The pore size is determined by the carbon chain length of the linker or the

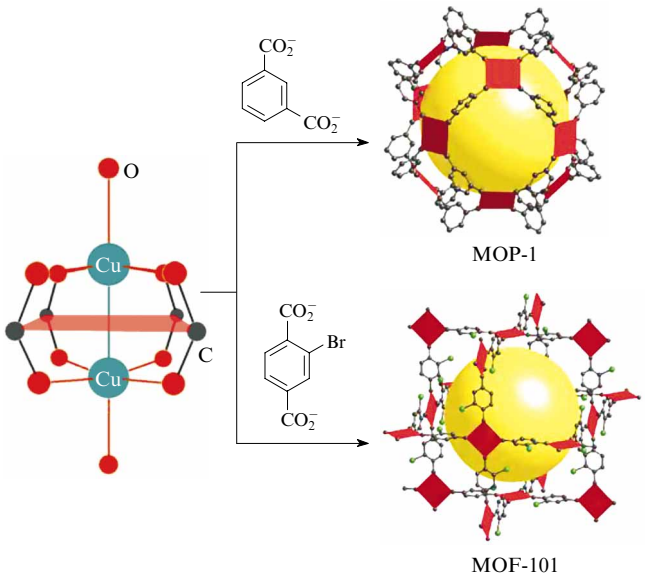

Figure 4. Examples of the change in the geometry of MOFs depending on the mutual arrangement of substituents in the linker molecule.[240–242]
Yellow spheres show the pore volumes.

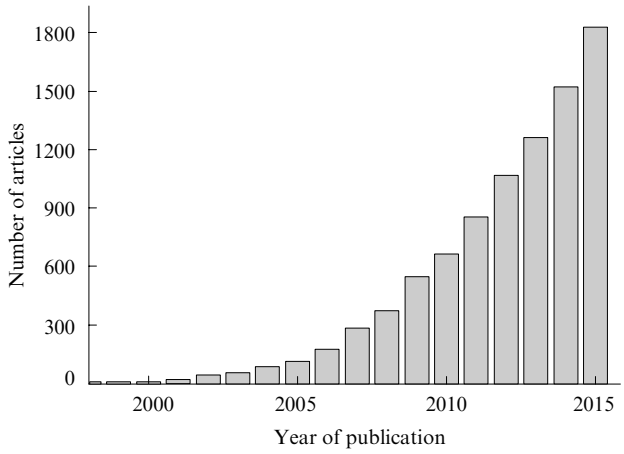

Figure 5. Diagram illustrating the dynamics of interest in MOFs (according to the Web of Science database).

number of benzene rings in it, whereas the introduction of different substituents and functional groups into the linker is responsible for the additional selectivity and unique chemical properties of the pores (Fig. 4).[150, 243–245]

A vast variety of building units and connection modes affords a great number of different MOFs. In particular, more than 20 000 MOFs have been reported and studied within the decade preceding the publication of Furukawa *et al.*[46] To obtain reliable statistics of the number of currently available crystal structures of MOFs, the Cambridge Crystal Database can be searched for polymer structures containing transition-metal atoms bonded to oxygen or nitrogen atoms. Such a search reveals 54 341 MOF structure (almost 7% of the total number of available compounds) as for May 2015. A search of the Web of Science database for articles addressing MOFs gives similar statistics and demonstrates increased recent interest in materials of this type (Fig. 5).

The MOF properties can be varied by selecting appropriate starting components. This has led to the creation of materials capable of selectively absorbing small molecules[194] or adding large species, for example, fullerenes C_{60} (Ref. 246) and even the protein myoglobin.[57] It is worth noting that not only the selection of structure constituents is important but also the manner in which they are connected together. Studying the formation of a framework from building units has revealed some regularities that can be used to predict the properties of synthesized MOFs.[230]

IV. Application of metal-organic frameworks

The MOF structures have a great potential for air purification from toxic gases.[77] For example, ammonia absorption can occur either through chemisorption on coordinatively unsaturated active sites, which causes in most cases the collapse of the framework, or through the formation of hydrogen bonds with functional groups of organic linkers. Such impurity removal mechanisms are also suitable for hydrogen sulfide. It is more challenging to remove sulfur and nitrogen dioxides as well as chlorine since they do not bind to coordinatively unsaturated active sites. In this case, the MOF pores should be functionalized for each specific task.

For purification of aqueous solutions, MOFs should be humidity-resistant. In particular, MIL-101 is able to remove Methyl Orange[247] and Xylenol Orange;[248] MOF-235 can remove not only Methyl Orange but also Methylene Blue[249] owing to electrostatic interactions between the dye and adsorbent molecules; MIL-100-Fe is proposed for removing Malachite Green.[250] Frameworks with large capacity and affinity for C_6-C_8 hydrocarbons can be used for removing oil spills. In particular, the fluorinated framework F-MOF-1 is able to reversibly adsorb n-hexane, cyclohexane, benzene and toluene, not adsorbing water at the humidity close to 100%. However, it should be emphasized that the extensive use of MOFs for filtration requires considerable sample preparation efforts. Many MOFs do not withstand high pressures during pelletization, since this leads to the collapse of their structure.

Different applications of MOFs were reviewed by Ryder and Tan.[251] In particular, some MOFs are used in the photocalytic hydrogen production.[252, 253] The MIL-101 material itself is not a semiconductor photocatalyst; however, its nanopores can accommodate CdS nanoparticles doped with 0.5% Pt.[254] Embedding of 5% or 10% CdS in MOFs increased the hydrogen evolution rate from zero to 22 and 150 mol h^{-1}, respectively.

The porous structure of MOFs is also considered as an electrolyte membrane that enables charge transfer from the cathode to the anode in fuel cells. The MOFs with good conductivity have been listed.[252, 255]

In modern lithium ion fuel cells based on the reversible lithium intercalation/deintercalation mechanism, the capacity of the cathode material ($LiCoO_2$) is 148 mA h g^{-1}, and the capacity of the graphite anode is 372 mA h g^{-1} (Ref. 256). To enhance the capacity of the cathode material, the MOF based on zinc formate $[Zn_3(HCO_2)_6]$ has been considered.[257] After a few cycles, the capacity of the active material was stabilized at 560 mA h g^{-1}.

Porous MOFs can be used as a matrix for synthesis of metal oxides,[258] quantum dots[259] and carbon composites with a high surface area.[260] The latter are of interest for new-generation fuel cells based on Li–S electrolytes. To enhance the electrical conductivity of the cathode material, it should be combined with highly porous carbon. A good candidate for use in this process is nanoporous carbon prepared, for example, by solid-state thermolysis of the MOF matrix. Meng *et al.*[261] described the preparation of a Co_3O_4 nanocomposite with a pore size of $\sim$10 nm *via* solid-state thermolysis of a cobalt-based MOF. Such a material is excellently suitable as supercapacitor electrodes, exhibits a specific capacitance of 150 F g^{-1} at a current density of 1 A g^{-1} and retains stability after 3400 cycles.

The electronic properties of MOFs can be tuned by varying the length of linker molecules. This is especially important for creation of novel Zn-based semiconductor materials.[262]

An attractive feature of MOFs for medical applications is their ability to controllably adsorb and desorb drugs. Liedana *et al.*[263] optimized the caffeine encapsulation by changing the properties of linkers — terephthalic acid — in MIL-88-Fe. A large surface area makes it possible to use MOFs for gas therapy in medicine, for example, for NO delivery.[264] MOFs can store gas molecules for months,

releasing them only when treated with water.[11] For medical applications of MOFs, the crystal size should be reduced to a few nanometres, which is currently a challenging task. Possible *in vivo* toxicity of high doses of nanoparticles of three iron oxide-based MOFs (MIL-88A, MIL-88B-4CH3 and MIL-100) was studied by evaluating their distribution, metabolism and excretion.[265] All studied parameters (serum, enzymatic, histological) are in agreement with a low acute toxicity. The MOFs degraded into components, and, hence, carboxylate linkers and an iron excess could be excreted from the body.

MOFs open up broad prospects for making a breakthrough in materials science.[46, 57] Further progress in synthetic chemistry can lead to creation of materials that (1) can count, sort and code information; (2) will have separate compartments with different properties linked together to function synergistically, for example, in catalysis of parallel reactions; (3) will be highly selective at a high reaction rate.[46]

V. Basic methods of synthesis of metal-organic frameworks

Different methods of synthesis of MOFs have been described: traditional synthesis (including solvothermal), microwave, electrochemical, mechanochemical and sonochemical. Commonly, MOFs are crystallized from a solution. Water and especially organic solvents fill the pores together with unreacted residues of the initial compounds. Thermodynamically, dense structures are more stable. Therefore, encapsulation of foreign molecules into the porous structure as well as the formation of inorganic units play a key role in the formation of MOFs. An important step is postsynthetic treatment of MOFs — purification and activation. Purification is of crucial importance for catalytic applications of MOFs, since impurities of reaction by-products can mimic the catalytic activity and considerably deteriorate the absorption possibilities. Purification usually consists of treatment with a solvent, often at elevated temperature. The activation of a material implies pore emptying, which is often a difficult task since removal of inclusions from a porous structure by heating can lead to collapse of the framework, especially if the guest molecules and the framework are bound by rather strong bonds or if inclusion removal requires high temperatures. There are different methods for simplifying the activation of MOFs. The most common among them is replacement of the solvent by a more volatile one, which makes it possible to decrease the treatment temperature.[220]

The reproducibility of synthesis results is of special importance. Because of the complex structure and the presence of pores and organic components, not only some deviations from the perfect model structure can be observed but also the structure and, hence, the properties of samples can vary from experiment to experiment. Similar changes in properties (in particular, in thermal stability) as the function of the initial component ratio (Zr : BDC : DMF) and temperature of synthesis have been studied by Shearer *et al.*[266] for MOF UiO-66 as an example. Another example of similar investigation was reported by Hafizovic *et al.*,[267] who studied the structure and properties of MOF-5 as a function of synthesis and postsynthetic treatment conditions.

Formation of MOFs is strongly affected by the solvent and the presence of different additives. When studying the synthesis of MOF-5, Li *et al.*[196] have revealed that the addition of triethylamine promotes the reaction of H_2BDC with zinc nitrate since it increases pH, which is favourable for acid deprotonation. A small addition of hydrogen peroxide facilitates the formation of O^{2-} ions, which are the centres of secondary metal–oxygen clusters.[196] Biemmi *et al.*[268] have studied the effect of different zinc sources, solvents and pH values on the possibility of solvothermal synthesis of MOF-5 and HKUST-1 (Fig. 6).

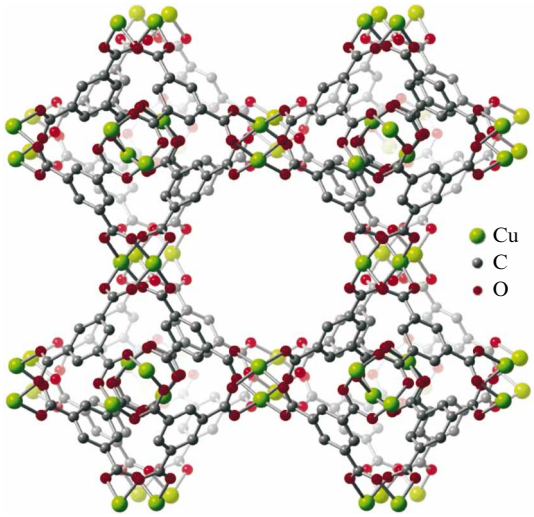

Figure 6. A fragment of the crystal structure of MOF HKUST-1 (the hydrogen atoms are omitted for clarity).[97]

It has been revealed that the use of copper and zinc acetates affords smaller crystals. The authors explain this fact by the change in nucleation rate during crystallization. In addition, as distinct from MOF-5, the change in acidity caused by the use of zinc acetate in synthesis of HKUST-1 leads to the formation of an unknown impurity phase. When chlorides are used, in none of the systems are solid products formed. This is attributed to the difference in solubility between chlorides and other salts, as well as to the tendency for complexation of chloride ions. It has been noted that a special role is played by an impurity of aromatic hydrocarbons in the solvent. Namely, a decrease in the polarity of the reaction mixture leads to a decrease in the yield of MOF-5 (and to an increase in the content of an unknown phase). At the same time, when zinc oxide is used, the MOF-5 phase forms at any ratio of the solvents. An additional introduction of H_3O^+ or OH^- ions leads to the formation of MOFs of two different compositions: $(H_2NEt_2)_2[Zn_3(BDC)_4]$ and $Zn_3(OH)_2(BDC)_2 \cdot 2H_2O$, respectively. For HKUST-1, conditions of synthesis of the phase free of copper oxide impurities have been optimized, and the effect of of the initial concentrations of the components on the morphology and size of resulting crystals has been studied.

Tranchemontagne *et al.*[269] have experimentally demonstrated that when $Zn(OAc)_2$ is used as the zinc source, it is unnecessary to additionally alkalify the reaction mixture.

V.1. Traditional synthesis

Traditional synthesis can be divided into two categories: solvothermal and non-solvothermal. The term solvothermal implies the use of any solvent and is more general than the term hydrothermal used where the solvent is water. Non-solvothermal synthesis occurs below the solvent boiling point in open flasks at atmospheric pressure, whereas solvothermal synthesis is carried out at the boiling temperature of the solvent or above this boiling point in special closed chemical reactors at elevated pressure caused by solvent vapour or produced by a pump.

Non-solvothermal synthesis does not require complex equipment, can be accomplished both at room temperature and on heating. A common scheme of such synthesis implies the choice of the salt (metal source), organic linker and solvent, as well as the adjustment of pH and temperature to provide the maximal yield of the target MOF. For a precipitate to form, the reagent concentrations should be selected in such a way that the nucleation conditions are achieved. This is usually promoted by increasing temperature and evaporating solvent. In addition, the concentration gradient can be created by slow cooling of the solution, solvent layering or slow diffusion of one of the reactants.[216]

Many known MOFs have been synthesized by this method. In particular, mere mixing of solutions without heating gave MOF-5,[196,270] MOF-74, MOF-177,[269] ZIF-8.[271] Cravillon *et al.*[272] have reported a modified procedure of synthesis of ZIF-8: changing the component ratio, the authors have managed to obtain the pure product without heating, excess pressure and ultrasonic or microwave treatment.

Huang *et al.*[273] have achieved the concentration gradient in synthesis of ZIF structures through the layering of the components. Imidazole derivatives were dissolved in methanol and were carefully, without mixing, poured onto a solution of $Zn(OH)_2$ in 25% aqueous ammonia.

Solvothermal synthesis affords higher yields and better crystallinity of the product. Owing to the elevated pressure, the solvent can be heated above its boiling point (at a pressure of 1 atm), which enhances the solubility of the salts involved in the reaction and promotes the reactions. In addition, slow crystallization from a solution leads to the formation of regular large crystals with a high internal surface area. Among the advantages of this procedure is the possibility of total control of synthesis conditions for a long period of time, which allows one to develop reproducible protocols. However, solvothermal synthesis requires special equipment (autoclaves or sealed containers that can withstand increased pressure); in addition, the duration of the process should be taken into account (the synthesis can continue for several weeks and even months).

In particular, Li *et al.*[274] have synthesized MOF-5 by three approaches: direct mixing of the reactants with Et_3N, slow addition of Et_3N and solvothermal synthesis. Figure 7 demonstrates a different degree of crystallinity of the prepared samples. The authors have emphasized that solvothermal synthesis affords samples with higher porosity. The Brunauer–Emmett–Teller (BET)[275] surface area of the sample synthesized through a solvothermal route was 839 $m^2\ g^{-1}$, and that of the samples prepared by the non-solvothermal method was 500.8 $m^2\ g^{-1}$. In addition, the solvothermal approach excludes the necessity of extra alkalization of the solution with triethylamine.

A similar approach has been used to synthesize the MOF UiO-67 with a degradation temperature of 540 °C (one of the highest characteristics of thermal stability among MOFs).[238] For synthesis, a solution of $ZrCl_4$ and terephthalic acid in DMF was used. This mixture was heated at 120 °C for 24 h.

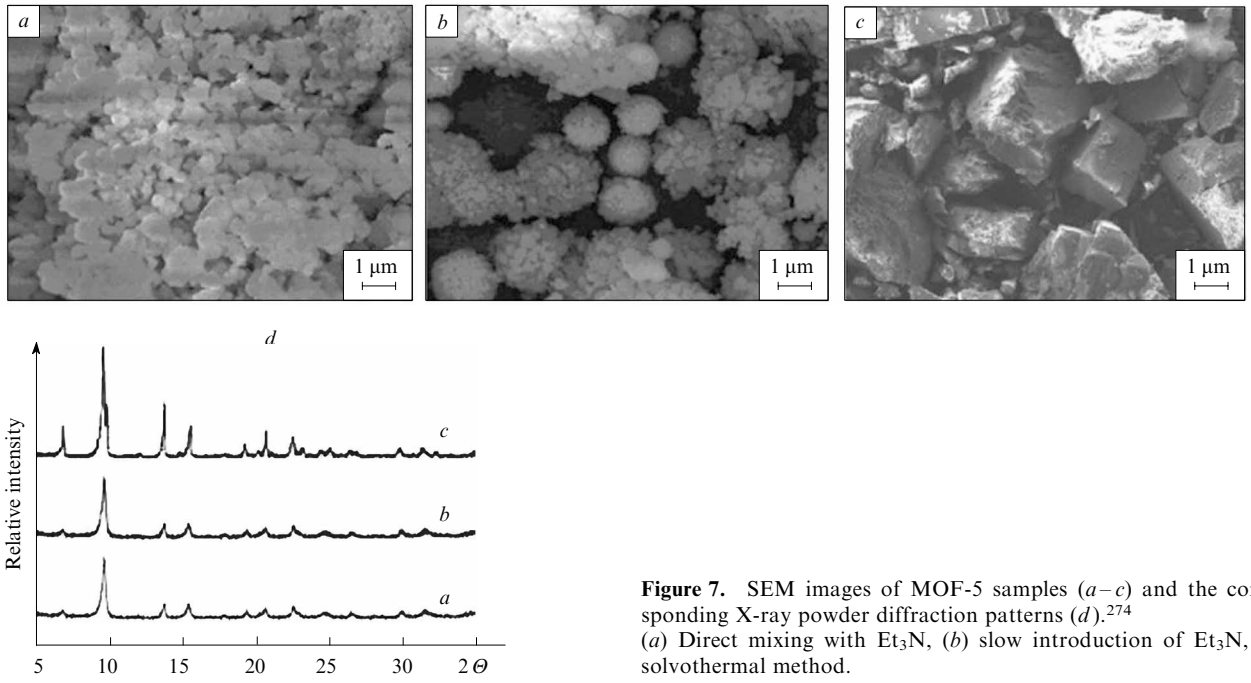

Figure 7. SEM images of MOF-5 samples (*a*–*c*) and the corresponding X-ray powder diffraction patterns (*d*).[274]
(*a*) Direct mixing with Et_3N, (*b*) slow introduction of Et_3N, (*c*) solvothermal method.

Table 2. Formulas and conditions of solvothermal synthesis of some MIL structures.

MOF	Formula (initial compounds)	T/°C	Time /h	Ref.
MIL-64	$Al_{10}(PO_4)_4(HPO_4)_6F_9(H_2O)_4 \cdot OH \cdot 2\,H_3N(CH_2)_3NH_3$ ($Al(OH)_3$, H_3PO_4, HF, $H_2N(CH_2)_3NH_2$)	180	720	276
MIL-69	$Al(OH)(O_2CC_{10}H_6CO_2) \cdot H_2O$ ($Al(NO_3)_3 \cdot 9\,H_2O$, naphthalene-2,6-dicarboxylic acid ($HO_2CC_{10}H_6CO_2H$), KOH)	210	16	277
MIL-74	$M_3Al_6(PO_4)_{12} \cdot 4\,(H_3NCH_2CH_2)_3N \cdot 17\,H_2O$ (M = Mg, Mn, Co) [$Mg(NO_3)_2 \cdot 6\,H_2O$ [or $MnCl_2 \cdot 4\,H_2O$, or $Co(NO_3)_2 \cdot 6\,H_2O$], $Al(OH)_3$, H_3PO_4, $(H_2NCH_2CH_2)_3N$]	180	36	278
MIL-116	$M_2(OH)_2[C_6(CO_2)_6] \cdot 2\,H_2O$ (M = Al, Ga or In) [$M(NO_3)_3$ (M = Al, Ga or In), benzenehexacarboxylic acid]	210	24	279
MIL-122	$M_2(OH)_2[C_{14}H_4O_8]$ (M = Al, Ga, In) [$M(NO_3)_3$ (M = Al, Ga or In), naphthalene-1,4,5,8-tetracarboxylic acid ($C_{14}H_8O_8$)]	210	24	280
MIL-37	$Fe(OH)(H_2O)(O_3P(CH_2)_2CO_2H)$ ($FeCl_3 \cdot 6\,H_2O$, $(HO)_2(O)P(CH_2)_2CO_2H$, NaOH)	170	24	281
MIL-38	$Fe^{II}_3(OH)_2(H_2O)_4(O_3P(CH_2)_2CO_2H)_2$ (Fe, $(HO)_2(O)P(CH_2)_2CO_2H$, NaOH)	170	48	282
MIL-49	$Fe^{III}(H_2O)(O_3P(CH_2)CO_2)$ (Fe, $(HO)_2(O)PCH_2CO_2H$, NaOH)	170	48	283
MIL-65	$[Fe^{II}_3(H_2O)_5(BTC)_2 \cdot 3\,H_2O]$ (Fe, VCl_3, H_3BTC, NaOH)	180	48	284
MIL-82	$[Fe^{III}(OH)[C_6H_2(CO_2)_2(CO_2H)_2] \cdot 0.88\,H_2O$ ($FeCl_2$, HF, $C_6H_2(CO_2H)_4$-1,2,4,5)	200	48	285

A solvothermal method has been used to synthesize differetnt structures with zeolite-like morphology, encorporating zinc (ZIF-1–4, 6–8, 10, 11) or cobalt (ZIF-9,12) and imidazole derivatives as linkers.[271] Many MOFs generally referred to as MIL (Materials of Institut Lavoisier) have been synthesized at the Lavoisier Institute in Versailles. The data on their synthesis are summarized in Table 2.

It is worth noting that products with different structures can be obtained by changing synthesis conditions. In particular, in 1998 Li *et al.*[195] reported the synthesis of the layered structure Zn(BDC)(DMF)(H_2O) through a non-solvothermal reaction of zinc nitrate and terephthalic acid; a year later, the same team of researchers synthesized a three-dimensional framework structure of cubic symmetry.[196]

V.2. Microwave synthesis

Microwaves (MW) are a form of electromagnetic radiation with frequencies between 300 and 300 000 MHz. Of the two components of radiation — electrical and magnetic, only the former has usually an effect on synthesis of compounds.[286] The maximal MW energy (0.037 kcal mol^{-1}) is insufficient for cleavage of chemical bonds in common organic compounds.[286] There are two types of MW impact on a substance that lead to heating: the action on polar molecules and on free ions. In both cases, polar molecules and ions try to align with the alternating field. In an electrolyte solution, electric current is generated and, hence, heating occurs due to resistance. In the case of polar molecules, for example, water, the resistance is caused by the presence of hydrogen bonds that prevent the dipoles from easily aligning with the variable field. There are many factors that influence the efficiency of this heating (dipole moment of a polar molecule, the possibility of its free rotation, *etc.*). For example, comparison of the effects of MW radiation on water in different physical states shows that the strongest effect is observed in the liquid state. In vapour, the effect of MW radiation is weak because of the absence of hydrogen bonds between water molecules (and, hence, the lack of heating due to resistance) and their low concentration. In solids, MW radiation is inefficient since reorientation of molecules firmly bound in the crystal lattice of ice is impossible.[287]

Numerous experiments have demonstrated that microwave treatment helps to essentially reduce the synthesis duration; however, the observed increase in reaction rates cannot be explained only by rapid heating. MW irradiation does not change the activation energy (which is a constant for each reaction) but provides energy to overcome the activation energy barrier. As a result, the reaction is completed in a shorter time than in the traditionally heated system. Noteworthy is yet another important factor responsible for the increase in the reaction rate and yield. The characteristic oscillation period for microwave radiation in which it transfers energy to the system is 10^{-9} s. The time required for transition of the molecule absorbing this energy from the excited state to equilibrium is $\sim 10^{-5}$ s. Thus, microwave radiation delivers energy to the molecule faster than it is able to transfer to a medium; therefore, the system is in a constant state of disequilibrium and has the enhanced reactivity.[286]

In any synthesis of MOFs, the choice of a solvent plays an important role. The use of microwave radiation imposes new specific requirement on the solvent. The solvent should absorb microwave energy and be able to convert electromagnetic energy into heat. To assess this ability, the dielectric loss tangent is used.

$$\tan\delta = \frac{\varepsilon''}{\varepsilon'}$$

where ε'' stands for dielectric losses, and ε' is the relative permittivity.[286] The larger the dielectric loss tangent, the more efficiently the solvent converts MW energy into heat.

Table 3. Dielectric loss tangent for some solvents (room temperature, 2450 MHz).[286]

Solvent	tan δ	Solvent	tan δ
Ethylene glycol	1.350	Water	0.123
Ethanol	0.941	Chlorobenzene	0.101
DMSO	0.825	Chloroform	0.091
Propan-2-ol	0.799	Acetonitrile	0.062
Propan-1-ol	0.757	Acetone	0.054
Formic acid	0.722	THF	0.047
Methanol	0.659	Dichloromethane	0.042
Acetic acid	0.174	Toluene	0.040
DMF	0.161	Hexane	0.020

The tan δ values for common solvents are presented in Table 3.

The penetration depth of MW radiation into a dielectric material should also be taken into account. It is designated as D_p and can be calculated by the equation

$$D_p = \frac{\lambda}{4\pi}\left[\frac{2}{\varepsilon'\left(\sqrt{1+(\varepsilon''/\varepsilon')^2}-1\right)}\right]^{1/2}$$

where λ is the wavelength.

Since both the dielectric permittivity and dielectric losses are temperature dependent, the penetration depth also depends on temperature; namely, it increases with increasing temperature.[287] In particular, for water at 25 °C, the penetration depth is 1.8 cm. Therefore, for efficient heating in a microwave oven, it is necessary either to use container of appropriate volume or to stir the heated sample.

Another specific feature of microwave heating is some increase in the boiling point of a solvent as compared with conventional heating; *i.e.*, as the boiling point is achieved and, usually, even above this temperature, the solvent does not boil, being in the metastable state. This phenomenon can be explained by the fact that a solution can boil only in contact with its vapour. As a rule, in addition to the upper boundary with air, similar contacts are formed on the imperfections of glass (or another material of a vessel), which cannot be wetted with the solvent. Thus, liquid solvent–vapour interfaces are formed on these imperfections, and it is precisely these areas where incipient bubbles of boiling form. However, in microwave heating, the vessel walls are the coldest areas of the system; hence, the only possible contact of the solvent with vapour is a small area on the boundary with air, the nucleation of bubbles is hindered, and the solution is overheated without boiling onset.[287]

Microwave radiation for synthesis of MOFs was used for the first time in 2005.[288] This method made it possible to reduce the time of synthesis of the MIL-100 framework from 96 (Ref. 289) to 4 h. MIL-100 was synthesized from chromium metal, H_3BTC and an aqueous solution of hydrofluoric acid. The reactants were mixed, placed into an autoclave and slowly heated to 220 °C, using conventional electrical heating[289] or microwave radiation.[288] In the latter case, MIL-100 was produced within 1 h; however, the impurity of chromium metal disappeared only after 4-h heating. It should be noted that the yield of the product after the 24-fold decrease in synthesis duration remains the same as in conventional hydrothermal synthesis. An isostructural analogue with iron instead of chromium was obtained even within 30 min of microwave irradiation.[290]

MIL-101 ($Cr_3F(H_2O)_2O[C_6H_4(CO_2)_2]_3$) with the terephthalate linker was synthesized in 2007, using microwave radiation.[291] Varying the heating time from 1 to 60 min, the authors found that long-term irradiation (60 min or longer) led to the appearance of an impurity phase. Four years later, there was published a study[292] on the influence of synthesis methods and conditions on the MIL-101 particle size. It has been demonstrated that microwave irradiation for 15 min produces crystals 50 nm in size in good yield. The isostructural compound with iron instead of chromium was synthesized for the first time by microwave treatment of solutions of iron chloride $FeCl_3$ and terephthalic acid in DMF for 10 min.[292] The synthesis of the related compound Fe-MIL-101-NH_2 in which aminoterephthalic acid acted as the linker has been reported by Taylor-Pashow *et al.*[290] The synthesis was carried out in a microwave oven for 5 min and gave crystals ~200 nm in size.

The effect of synthesis conditions, namely, temperature and method of heating, on the MOF structure has been studied.[293] The synthesis of the MOF of general formula $Cu_3(BTC)_2$ has been described. In particular, synthesis at 120 °C leads to the $Cu_3(BTC)_2(H_2O)_3$ phase, whereas synthesis at 170 °C with the use of microwave radiation gives the $[Cu_2(BTC)(OH)(H_2O)]\cdot 2H_2O$ phase.

V.3. Electrochemical synthesis

The key idea of the electrochemical synthesis of MOFs is that metal ions are introduced not from a solution of the corresponding salt or through the formation of these ions during the reaction of a metal with an acid, but as a result of electrochemical process. Namely, metal ions are supplied in the reaction mixture containing dissolved linker molecules and an electrolyte through the dissolution of anode. This makes it possible to avoid the formation of anions in the course of reaction and to initiate a continuous process, which is essential for going to the production of relatively large amounts of MOFs.[216]

To prevent metal cations from depositing on the cathode, protic solvents are used; however, in this case, hydro-

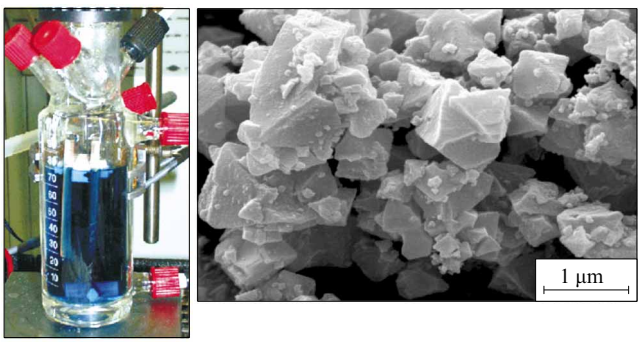

Figure 8. Setup for electrochemical synthesis of MOF HKUST-1 (*a*) and SEM image of the product (*b*) (magnification, 20 000).[294]

gen can be released in the course of electrochemical process. At the same time, some solvents, such as acrylonitrile, acrylates and maleates, are the first to be reduced, and with small amounts of these solvents the above problem is avoided.

The electrochemical method was used for the first time to synthesize MOFs (HKUST-1) in 2005 (Fig. 8).[294] As the dissolving anode, copper sheets 5 mm thick were used; the sheets were dipped in a solution of H_3BTC in methanol together with copper cathodes. Within 150 min after applying voltage, a green-blue precipitate was deposited.

A somewhat modified method was proposed by Hartmann *et al*.[295] They compared the hydrothermal, conventional non-hydrothermal and electrochemical methods of synthesis of HKUST-1. All methods gave the $Cu_3(BTC)_2$ phase with comparable surface areas and pore volumes.

It should be especially noted that this method affords both powders and films. For example, a thin layer of HKUST-1 was electrochemically deposited on copper mesh used as anode.[296]

V.4. Mechanochemical synthesis

Mechanochemistry studies reactions between solids usually initiated only by means of mechanical energy, for example, by milling in ball mills. This approach has become especially popular since it allows carrying out reactions rapidly and in high yield without solvent or with its small amount. Currently there is no general theory explaining physicochemical processes that occur in mechanochemical reactions. The most popular approaches are the hot-spot model and the magma–plasma model. The former model considers the contact of two solid surfaces exposed to mechanochemical treatment. Local distortions of the ductile material surface with an area of ~ 1 m^2 lead to a sharp increase in temperature (> 1000 °C) at this spot, which lasts for a short period of time (10^{-3}–10^{-4} s). For brittle materials, somewhat different processes leading to local heating are considered, namely, formation of hot spots at the ends of propagating cracks.

The magma–plasma model focuses on the processes that occur directly at the contact spot of colliding particles. According to this model, the local temperature at such spots can exceed 10^4 °C owing to the instantaneous formation of plasma and large energy release, including emission of free electrons.[297] It seems like that these theories are inapplicable to the mechanochemical synthesis of MOFs since such high temperatures would lead to the decomposition of the initial organic components and the product. However, a strictly local character of such temperature bursts and their extremely short duration can initiate reactions between milled components rather than lead to their degradation. The presence of a liquid component in the course of mechanochemical reaction offers additional advantages: easier crystallization, higher degree of crystallinity of the reaction product and higher yield of the target product due the higher mobility of the reactants.

In addition, continuous milling of components promotes diffusion and permanently forms new surfaces with enhanced reactivity.[298] For the synthesis of MOFs, this method was used for the first time in 2006.[299] The authors mixed copper acetate and isonicotinic acid (HINA) in a ball mill for a few minutes. This procedure led to a rather well-crystallized product with the formula $Cu(INA)_2 \cdot x\,H_2O \cdot y\,AcOH$. Both the water and acetic acid located in MOF pores were the reaction products and were removed on heating.

Two years later, the same research team reported the results of an array-based study of the possibility of mechanochemical synthesis of different MOFs. The metal, the mode of introduction of it, the linker, the solvent and synthesis conditions were varied.[300]

HKUST-1 has synthesized by the mechanochemical method in 2010.[301, 302] In both studies, copper acetate and H_3BTC under solvent-free conditions have been used. Yuan *et al*.[301] pay attention to the fact that whereas the formation of $Cu(INA)_2$ occurs almost spontaneously (milling for 1 min is sufficient), formation of HKUST-1 requires longer mixing time. In addition, small amounts of acetic acid (added in the mixture for milling or generated in the course of reaction) sharply increase the formation rate of $Cu(INA)_2$ rather than HKUST-1. The authors believe that this can be related to the higher porosity of HKUST-1. Instant absorption of liquid components completely rules out their participation in dissolution and any other effects on the reaction mixture.

V.5. Sonochemical synthesis

The impact of ultrasound on liquid and colloid systems is mainly caused by cavitation. This is a phenomenon of vapour formation and air release caused by a decrease in pressure in a liquid as a high-intensity acoustic wave propagates through it. Theoretically, a liquid starts boiling when the pressure in some regions of the flow is reduced to its saturated vapour pressure. However, actually, the decrease in pressure leads to the release of dissolved air from liquid and formation of gas voids, cavities. The pressure in cavities is higher than the saturated vapour pressure. Thus, the cavity starts forming from a nucleus, increases to a finite size and, then, collapses. The whole process takes only a few milliseconds. The nuclei for cavity formation are microscopic bubbles. They form in tiny cracks on the vessel surfaces and (or) at the interfaces of suspended particles. When bubbles collapse, there is observed a faint glow caused by the heating of the gas in a bubble induced by high pressure. Thus, the bubble collapse leads to a significant increase in temperature and high pressure differences in the liquid surrounding the bubble.[303] As applied to chemical processes, the use of ultrasonic waves and, in particular, cavitation has several important effects. First of all, resonant bubbles act as an agitator, increasing the area of the contact between the reagents. In addition, thermal impact and pressure differences lead to disintegration of particle aggregates, which also increases the contact area. However, sonication can also lead to more serious changes, for example, to removal of adsorption and solvation shells from the surface of materials, bond rupture in polymer chains, formation of surface sites with uncompensated physical and chemical bonds; such sites are able to actively interact with molecules of chemical compounds. It should be taken into account that volatile solvents are usually insufficient for this method of synthesis since the high solvent vapour pressure inside the bubbles mitigates the effects that accompany bubble implosion.

For the first time, sonication was used for synthesis of a MOF (namely, $Zn_3(BTC)_2$) in 2008:[304] zinc acetate and H_3BTC were mixed in 20% ethanol and subjected to sonication for a few minutes (up to 90 min). However,

rather high yield of the product (75.3%) was achieved even after 5-min sonication.

In the same year, the use of sonication allowed Son *et al.* to decrease the time of synthesis of MOF-5 from 24 h (conventional heating) to 75 min.[305] Solutions of zinc nitrate and terephthalic acid in 1-methyl-2-pyrrolidone were mixed in an nitrogen atmosphere; then, the mixture was transferred into a reactor and subjected to sonication for 10–75 min. Precipitation of MOF-5 commences even after 8 min of sonication.

In addition, this method afforded $Cu_3(BTC)_2$ (HKUST-1) from an aqueous solution of copper acetate and a solution of H_3BTC in a mixture of DMF with ethanol.[306] The starting compounds were placed into a container mounted in a water bath and were subjected to sonication at a frequency of 40 kHz for some time (from 5 to 60 min). The yield of the product was from 62.6% to 85.1% depending on the synthesis duration.

Schlesinger *et al.*[307] compared six different methods of synthesis of HKUST-1: synthesis at atmospheric pressure with heating under reflux, solvothermal synthesis, electrochemical synthesis, microwaving, mechanochemical synthesis (with addition of a solvent) and sonication. All procedures gave the pure phase of the product. Maximal yield at minimal synthesis duration was achieved by means of microwave radiation.

VI. Functionalization of metal-organic frameworks

MOFs with a large surface area of pores is a convenient platform for designing functional materials tailored for solving specific problems in catalysis, gas separation and power engineering. Therefore, functionalization of MOFs is still one of the most topical problems attracting much attention of researchers (see, *e.g.*, Refs 47, 62, 154, 212, 215, 308–315). By the number of publications, this problem is even more important than optimization of existing methods of synthesis and design of novel structures. The metal sites of MOFs have no more than one coordination vacancy (after removal of the solvent), which limits the applicability of these materials, for example, in catalysis, where at least two coordination vacancies are required.

There are two basic approaches to functionalization of MOFs:

— the use of linkers containing functional groups in synthesis of MOFs;[189, 244, 316–319]

— postsynthetic modification of MOFs.

The latter approach involves, for example, insertion of complexes [(arene)tricarbonylchromium or -molybdenum $[-C_6H_4\{M(CO)_3\}-]$; M = Cr, Mo] into the linker through the reaction with corresponding metal carbonyls;[243, 320, 321] click reactions of the azide groups of MOFs with terminal alkynes,[182, 322] reduction of the aldehyde functional group of the ligand — imidazole-2-carbaldehyde — with sodium borohydride to obtain the alcohol functional group and its further reduction to the imine functional group by the reaction with ethanolamine,[323] the introduction of NH_2 groups through the reaction with nicotinoyl chloride,[185] formation of the NHAc group or longer amide chains through the reaction of the amino group with different acyl anhydrides,[244, 245, 324] metallation of organic linkers containing nitrogen atoms,[319, 325] functionalization with carboxy groups[326] and amino groups,[327–329] introduction of metal nanoparticles into MOF cavities.[173, 174, 176, 330–333]

Postsynthetic modification of a material makes it possible to create new and activate existing catalytic sites. New catalytic sites can be obtained by introducing noble metal nanoparticles into MOF pores, changing the ligand environment of metal sites or modifying organic linkers. Nanoparticles encapsulated into MOFs exhibit enhanced stability, high dispersion, controlled size and shape and do not prone to agglomeration as distinct from particles in an aqueous solution. The crystal lattice of MOFs can be an inert solid matrix and have an effect on reactivity and selectivity only due to the creation of steric hindrances. Or, conversely, MOF can directly participate in the catalytic process, for example, providing acidic or basic sites at the metal atoms or organic linkers. The pores of functionalized MOFs can be used as nanoreactors for polymerization reactions. In this case, polymer parameters, such as molecular mass and stereoregularity, as well as the sequence of comonomers in polymers, are controlled.[334]

MOFs with encapsulated metal nanoparticles are studied, first of all, by transmission electron microscopy (TEM). The stability of the crystal structure after exposure to electron beam and introduction of impurities are determined by X-ray powder diffraction. Absorption of molecules, for example, CO, is evaluated using Fourier transform IR spectroscopy. The surface-plasmon-resonance effect of noble metal nanoparticles is observed by optical spectroscopy methods. During these studies, it is essential to control the stability of synthesized structures of MOFs with nanoparticles. As distinct from zeolites, MOFs are strongly prone to dehydration when exposed to the electron beam of a microscope. This can be accompanied by both degradation of the MOF structure and agglomeration of nanoparticles in it.[335]

Figure 9 shows two approaches to the encapsulation of active entities in MOFs: the ship-in-a-bottle approach (synthesis of active sites into the pores) and, conversely, the

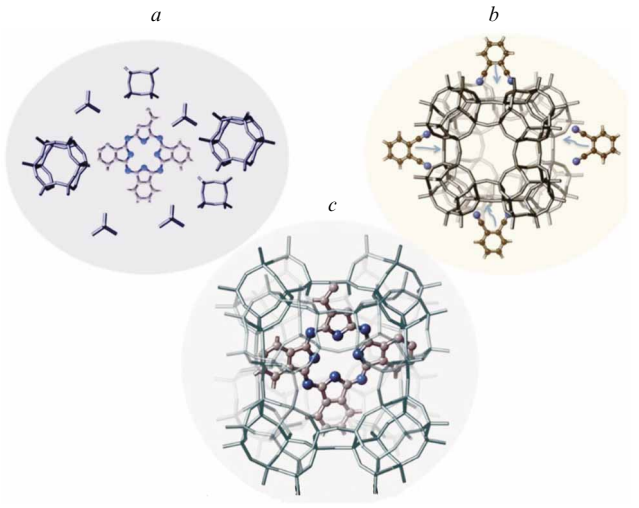

Figure 9. Two approaches to the synthesis of MOFs with new active sites in the pores (*c*): the bottle-around-a-ship (*a*) ship-in-a-bottle (*b*) methods.[332]

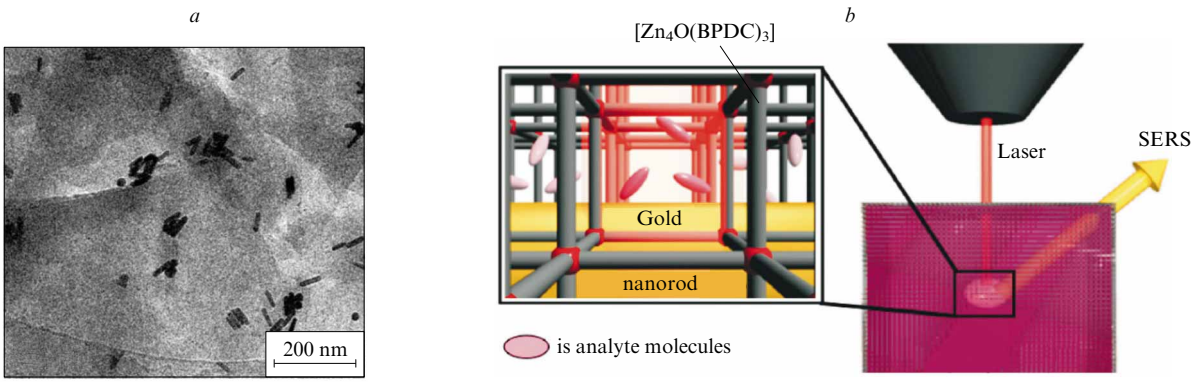

Figure 10. Synthesis of the MOF $[Zn_4O(BPDC)_3]$ around gold nanorods (*a*) and application of the resulting structure in SERS spectroscopy (*b*).[336]

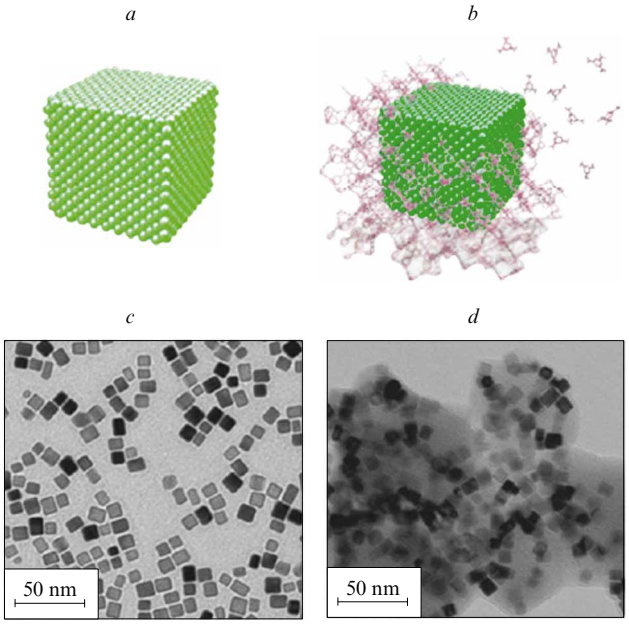

Figure 11. Models (*a*, *b*) and TEM images (*c*, *d*) of pure palladium nanoparticles (*a*, *c*) and particles covered with the MOF HKUST-1 (*b*, *d*).[337]

bottle-around-a-ship approach (synthesis of the MOF structure around active entities).

Figure 10 shows an example of realization of the second approach where the MOF $[Zn_4O(BPDC)_3]$ was synthesized in a solution of 11-mercaptoundecanoic acid-capped gold nanorods.[336] The resulting MOF crystals contained embedded gold nanorods and were used in surface-enhanced Raman scattering (SERS) spectroscopy.

Another example of realization of the bottle around a ship approach has been described by Li *et al.*[337] The HKUST-1 structure was synthesized in a solution containing palladium nanoparticles. It turned out that the hydrogen gas absorption of the resulting composite (Fig. 11) was 74% higher than that of bare palladium nanoparticles. The hydrogen uptake rate was also enhanced by the MOF coating of Pd nanoparticles.

The porous structure of MOFs can be used for target drug delivery. Magnetite Fe_3O_4 microspheres have been proposed for control of drug delivery.[338] The surface of Fe_3O_4 microspheres was modified with thioglycolic acid, and then these microspheres were successively immersed into a copper acetate solution in ethanol and into benzene-1,3,5-tricarboxylic acid (H_3BTC) at 25 °C. Figure 12 shows the TEM image of a microsphere covered with porous MOF after 30 cycles of successive immersion into solutions.

However, this approach is most often used for synthesis of MOFs around porphyrins or metalloporphyrins. These molecules are prone to dimerization and aggregation, but are stabilized when encapsulated into MOF pores.[339] Examples of molecules encapsulated into MOF pores by the bottle-around-a-ship procedure have been reported.[332]

For the introduction of noble metal nanoparticles into MOFs, the ship-in-a-bottle method in most frequently use. MOFs functionalized with nanoparticles are commonly have low catalytic activity because of diffusion limitations and are prone to degradation. However, the situation is radically changed if a definite nanoparticle size and morphology are essential in the catalytic reaction. In particular, in cross-coupling reactions, precise control of particle size, dispersion and polarity of the surrounding MOF structure makes it possible to achieve high catalyst activity and reaction selectivity.[331,340] Palladium nanoparticles 1.9 nm in size were synthesized in MIL-101(Cr) after impregnating it with a solution of $Pd(NO_3)_2$ in DMF.[340] The resulting catalyst was tested in the Suzuki–Miyaura reaction with participation of different aryl chlorides. The high catalytic activity was retained after, at least, five cycles and, for most chlorinated reagents (for example, chloroanisole), was higher than that of the commercial Pd/C catalyst.

MOF-5 was functionalized with ruthenium and had a surface area of 860 $m^2\ g^{-1}$.[341] The ruthenium concentration was as high as 30 mass %. Solid-state ^2H NMR has demonstrated weak interaction of embedded Ru nanoparticles with the MOF matrix. When oxygen is passed through the MOF, ruthenium nanoparticles are oxidized to RuO_2, which is a good catalyst for oxidation in air of different alcohols (Scheme 1). However, in the presence of RuO_2@MOF-5, the conversion of benzyl alcohol into benzaldehyde was only 25%, and the X-ray powder diffrac-

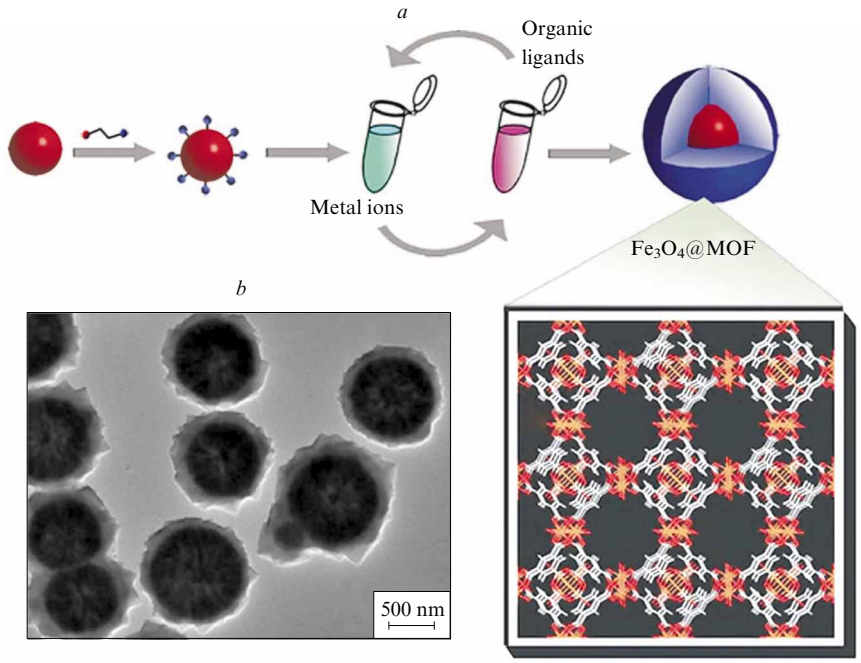

Figure 12. Scheme of synthesis of the porous MOF shell around Fe_3O_4 microspheres (*a*) and TEM image of nanoparticles obtained after 30 cycles of immersion into solutions (see text).[338]

tion pattern showed the degradation of the crystal structure of MOF-5. This unsatisfactory result is attributed to the stoichiometric formation of H_2O during oxidation and to the fact that MOF-5 is very sensitive to the presence of water. The RuO_2@MOF-5 composite has also been tested as a solid catalyst in hydrogenation of benzene to cyclohexane (3 atm H_2, 348 K); however, a conversion of only 25% has been achieved.

Scheme 1

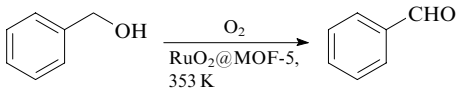

Huang *et al.*[331] have synthesized palladium nanoparticles in the MIL-53(Al) framework by means of direct ion exchange and subsequent reduction with $NaBH_4$. The resulting nanoparticles with an average size of 2–3 nm (Fig. 13) have been stabilized by the amino groups of the organic linkers of the MOF. They exhibit high activity and stability in the Suzuki–Miyaura reaction.

Different approaches to synthesis of nanoparticles inside MOFs have been reviewed by Meilikhov *et al.*[342] High concentrations of metal nanoparticles inside the porous MOF-5 structure can be achieved by loading it with metal organic vapour deposition precursors $[(\eta^5\text{-}C_5H_5)Cu(PMe_3)]$, $[MeAu(PMe_3)]$ and $[(\eta^5\text{-}C_5H_5)Pd(\eta^3\text{-}C_3H_5)]$.[330] The grinding of a solid MOF with noble-metal precursors with the subsequent annealing in a hydrogen flow is also used. This method have enabled the fabrication of gold nanoparticles in several matrices {MOF-5, HKUST-1, [Al(OH)(BDC)], ZIF-8, CPL-1 and CPL-2}, with $[Me_2Au(acac)]$ complex as the gold source (acac is acetylacetonate).[343] Figure 14 shows the distribution of gold nanoparticles inside the MOF MOK Au/Al-MIL-53. Gold nanoclusters <2 nm make possible

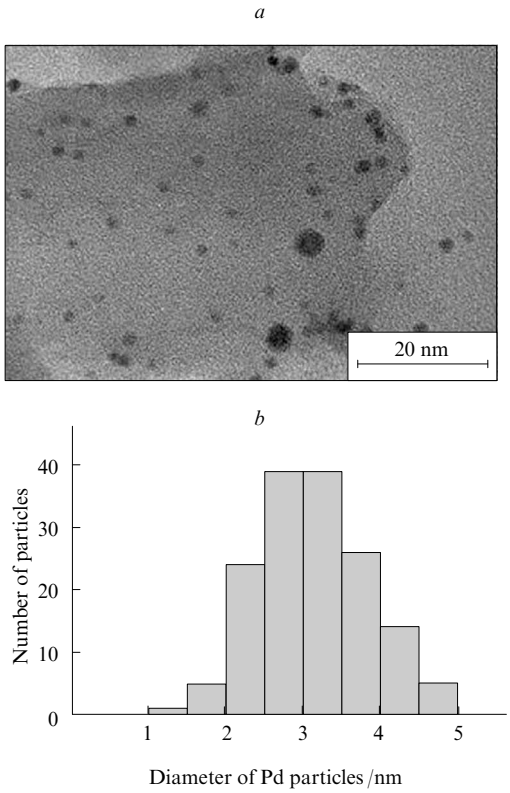

Figure 13. Dark-field TEM image of Pd nanoparticles in the MIL-53(Al) framework (*a*) and size distribution histogram of palladium nanoparticles in the framework (*b*).[331]

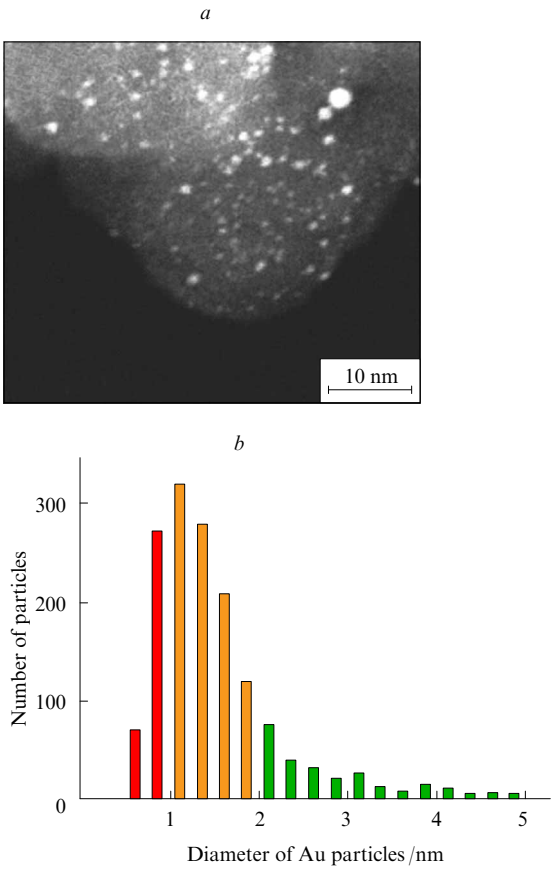

Figure 14. Dark-field TEM image of Al-MIL-53 functionalized with gold nanoparticles (*a*) and the size distribution of these nanoparticles (*b*).[343]

the one-pot synthesis of secondary amines from primary amines through successive oxidation and reduction with hydrogen. These clusters also stimulate the N-alkylation of aniline in the presence of benzyl alcohol without oxygen and hydrogen. The hydrogenation of imines to amines is also essentially promoted in the presence of gold nanoclusters < 2 nm.

The MOF matrix can be impregnated with a solution of a noble-metal salt, and then a reducing agent — hydrazine or sodium borohydride — can be introduced. A metal salt can be reduced by a MOF itself without using a reducing agent and a surfactant, as described by Cheon and Suh.[344] Hwang *et al.*[345] have functionalized coordinatively unsaturated metal sites (rather than the ligands) on the pore surface of dehydrated MIL-101(Cr), for example, with ethylenediamine; after treatment with hydrochloric acid, chloride ions are exchanged for the $[PdCl_4]^{2-}$, $[PtCl_6]^{2-}$ or $[AuCl_4]^-$ anions. At the final stage, noble metals are reduced by $NaBH_4$. Nanoparticles inside MOFs can be obtained by decreasing the amount of a nonaqueous solvent to a minimum (incipient wetness impregnation) and using a hot hydrogen flow as a reducing agent.[346]

Conversely, the MOF structure can be formed around pre-synthesized synthesized nanoparticles.[347] For example, the HKUST-1 framework composed of Cu^{2+} ions and benzene-1,3,5-tricarboxylate linkers has been synthesized on 11-mercaptoundecanoic acid-capped gold nanoparticles (Fig. 15).

Stable porous and phosphorescent MOFs composed of dicarboxylate ligands obtained from $[Ir(PPY)_2(2,2'\text{-BPY})]^+$ (PPY is 2-phenylpyridine, 2,2′-BPY is 2,2′-bipyridine) and secondary building units $Zr_6(\mu_3\text{-}O)_4(\mu_3\text{-}OH)_4(\text{carboxylate})_{12}$ can be functionalized with platinum nanoparticles through photooxidation of K_2PtCl_4 (Ref. 253) and used in photocatalysis (Fig. 16). Their efficiency is five times higher than that of analogous systems; in addition, they can be recycled and repeatedly used.[253]

To extend the scope of application of MOFs, organic linkers connecting secondary building units are functionalized. The introduction of OH, CHO, CO_2H, CN, N_3, $NAlk_2$, SH, $PAlk_2$, *etc.* groups is of practical interest. However, at the stage of solvothermal synthesis of MOFs, the presence of these functional groups can make the formation of the crystal structure itself difficult or impossible, for example, because these groups are able to coordinate metal ions. Therefore, MOFs are usually functionalized *via* postsynthetic modification. Chemical methods of chemical modification of linkers incorporated in MOFs have been reviewed by Cohen.[215]

Scheme 2 shows the modified linker — 2-aminotereph-thalate — in rare earth LIC-1 (abbreviated from Leiden Institute of Chemistry).[348] The LIC-1 powder was treated with ethyl isocyanate or acetic acid vapour for 1 h at 120 °C. The thus-modified organic linkers contain new functional groups. According to X-ray crystallographic data, the degree of substitution was $>40\%$ for LIC-F1 and $\sim 50\%$ for LIC-F2.

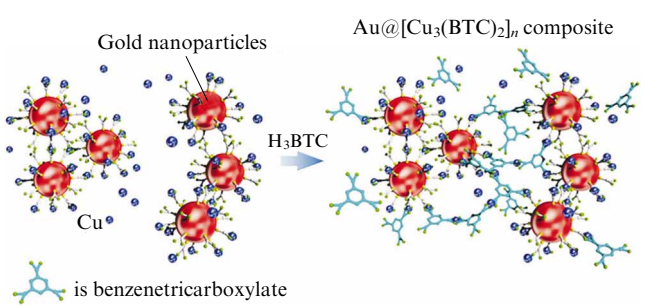

Figure 15. Self-assembly of the $Au@[Cu_3(BTC)_2]_n$ composite based on 11-mercaptoundecanoic acid-capped gold nanoparticles.[347]

Scheme 2

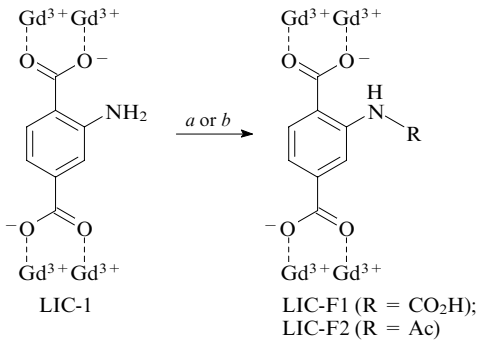

(*a*) EtNCO, H_2O, $-EtNH_2$ (R = CO_2H);
(*b*) AcOH, $-H_2O$ (R = Ac)

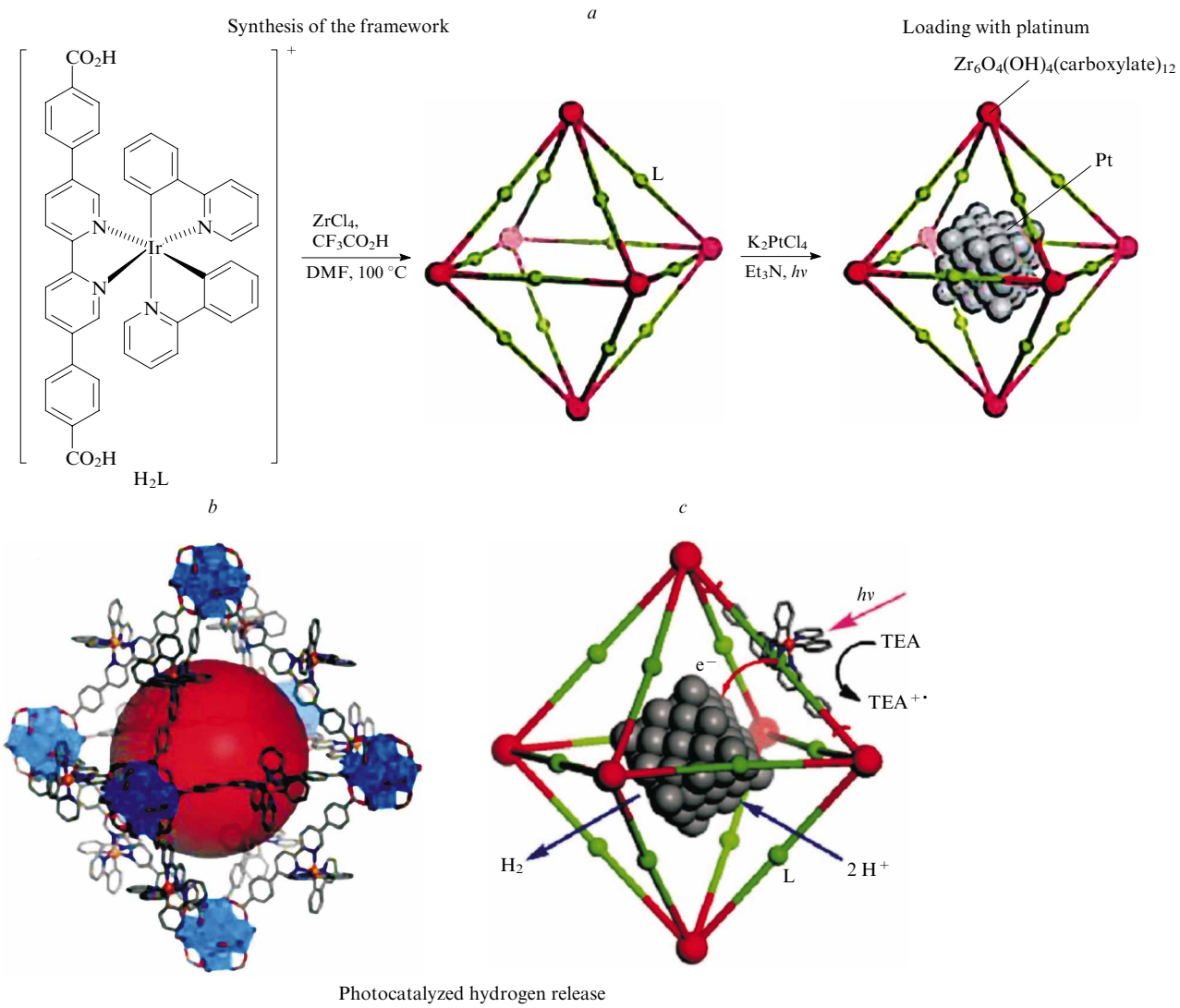

Figure 16. Scheme of synthesis and functionalization of the MOF $[Zr_6(\mu_3\text{-}O)_4(\mu_3\text{-}OH)_4(H_2L)_6(CF_3CO_2)_6 \cdot 64\,DMF]$ with platinum nanoclusters (*a*), the octahedral cavity in the framework (*b*) and the scheme of hydrogen evolution (light-induced electron transfer from the framework to the platinum nanoparticles leads to the reduction of hydrogen ions to release H_2) (*c*).[253]

MOFs isomorphous to zeolites are more stable than the other MOFs. The ZIF-90 phase was synthesized from 2-formylimidazolate and a Zn^{II} salt;[349] the structure contained reactive aldehyde groups. The resulting MOF was modified by two methods: it was placed either into a solution of $NaBH_4$ in methanol at 60 °C, which led to the reduction of aldehyde to alcohol in 80% yield (Scheme 3, ZIF-91), or into a solution of ethanolamine in methanol at 60 °C, which led to the formation of hydrazone moieties (see Scheme 3). Both new structures retained high crystallinity inherent in the initial ZIF-90, which was confirmed by X-ray powder diffraction. The presence of OH groups in ZIF-91 has been demonstrated by ^{13}C CP/MAS NMR, and the imino groups in ZIF-92 have been detected by Fourier transform IR spectroscopy. Thus, covalent modification of linkers using reducing agents or amines can be carried out in the as-synthesized MOF. Polar solvents and elevated temperature prevent such a reaction with chemically less stable MOFs.

Scheme 3

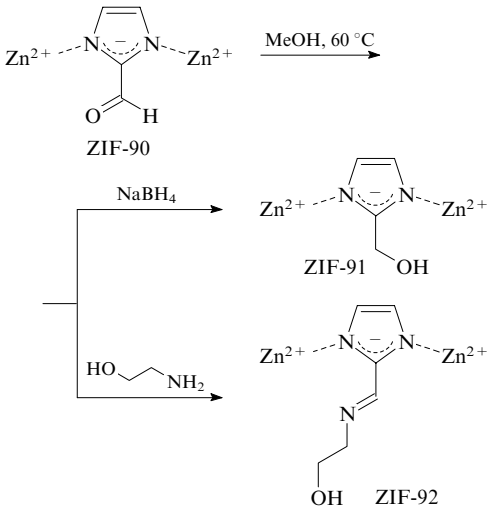

Scheme 4

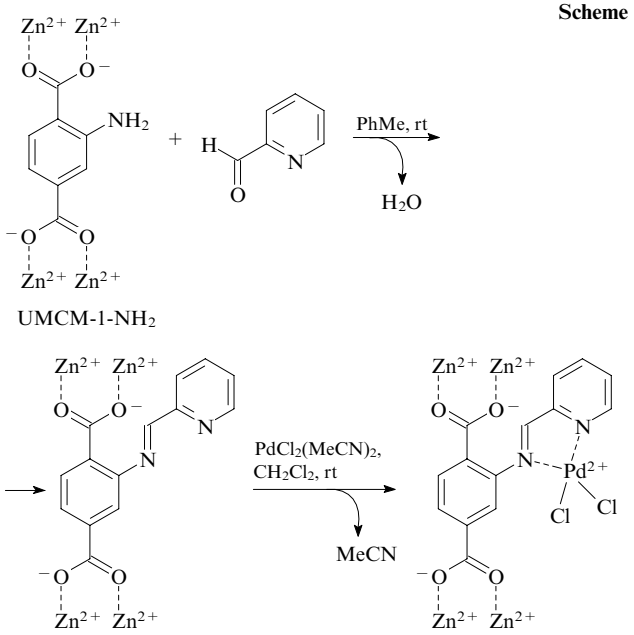

Doonan *et al.*[325] have also used the condensation of amino group with aldehyde to modify the ligands in MOFs. Compound UMCM-1-NH_2 was mixed with pyridine-2-carbaldehyde in toluene. The reacted lasted 5 days to give iminopyridine moieties in yield 87% (Scheme 4). At the next stage, the resulting product was treated with the $PdCl_2(MeCN)_2$ complex in dichloromethane to form palladium chelates in yield 85% (which was accompanied by a change in the reaction mixture colour from yellow to violet). The Pd K-edge EXAFS spectra have shown that the environment of Pd in the MOF — a square complex with two Pd–Cl and two Pd–N bonds (2.28 and 1.99 Å, respectively; the N atoms are from the iminopyridine moiety) — is different from the Pd environment in the initial $PdCl_2(MeCN)_2$.

VII. Traditional methods of analysis of metal-organic frameworks

The choice of the method of analysis of MOFs is dictated by their periodic structure, sensitivity to high temperatures (350 °C for MOF-5) and large surface area.

The most important characteristics of MOFs are precisely the high specific surface area and porosity, which are superior to the analogous characteristics of silica gels, zeolites and activated carbons. The specific surface area of MOFs is determined by the Brunauer–Emmett–Teller method,[275] which is in essence a development of the Langmuir theory for polymolecular (multilayer) adsorption. The method consists of measuring the experimental dependence of adsorption on pressure at constant temperature, from which the total surface area of the adsorbent is determined. For more detailed analysis of porosity (size distribution of pores) of samples from adsorption isotherms, additional calculation models are used.

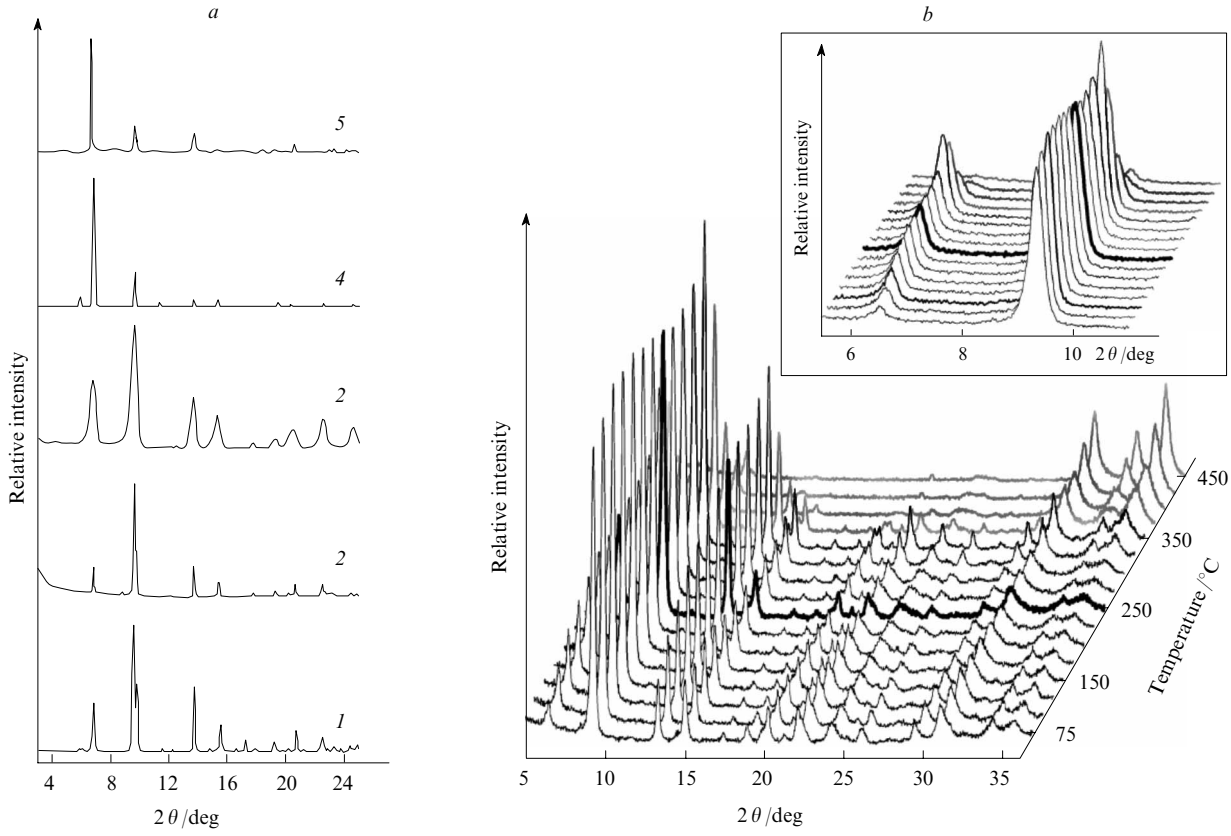

Figure 17. X-ray diffraction patterns for MOF-5 synthesized by different methods (*1–3*, *5*) and the calculated pattern for MOF-5 (*4*) (*a*); X-ray diffraction patterns for MOF-5 recorded on heating (*b*).[267]
The thick line shows the pattern corresponding to complete removal of the solvent (250 °C for MOF-5).

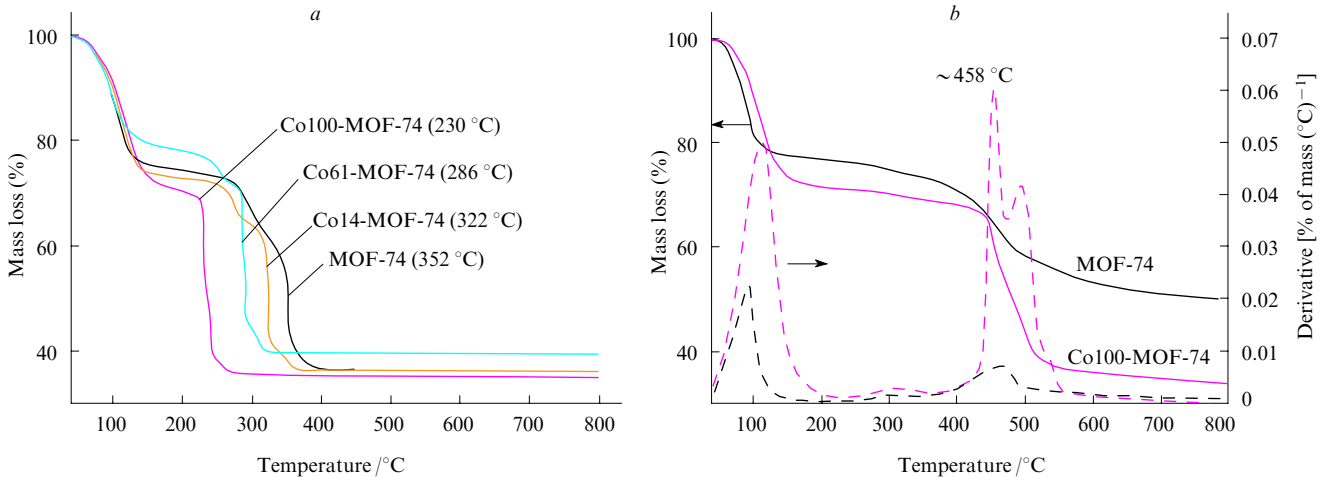

Figure 18. TGA curves for as-synthesized MOFs in air (*a*) and in a nitrogen atmosphere (*b*).[350]
The temperatures of degradation of organic ligands are parenthesized (*a*), and the dashed lines show the differential TGA curves (*b*).

Owing to the periodic structure of MOFs, the most common method for analysis of their structure is X-ray diffraction (XRD). However, since it is not always possible to grow an MOF crystal of appropriate size and quality, powder X-ray diffraction (PXRD) at room temperature is often used (Fig. 17 *a*). PXRD patterns allow a conclusion concerning the reproducibility of synthesis results or, conversely, make it possible to explain structural differences between the samples of the same MOF prepared by different methods.[267] Taking into account large unit cell parameters of MOFs and high electron density on metal sites, it can be a challenge to determine the structure composed of organic linkers by powder X-ray diffraction. An alternative method can be neutron diffraction, which also has some limitations. On the one hand, measurements can require considerable amounts of a sample, which is critical for testing new procedures of synthesis; on the other hand, organic linkers contain a large amount of hydrogen atoms, which should be replaced by expensive deuterium for methodical reasons.

Thermal stability is an important characteristic of MOFs, which are essentially inferior to zeolites in this respect. Heating MOFs to definite temperature induces evaporation of the solvent used in synthesis. In particular, DMF is completely removed from MOF-5 at 250 °C, which is not, however, reflected in X-ray powder diffraction patterns (see Fig. 17 *b*). On further heating above critical temperature (350 °C for MOF-5), the MOF structure starts to disintegrate: organic molecules are evaporated, and metal-containing secondary building units are converted into metal oxides. The thermal stability of MOFs and the effect of guest solvent molecules on their structure are studied by variable-temperature X-ray diffraction.

A direct method for studying the thermal stability of MOFs is thermogravimetric analysis (TGA), which measures the mass of the analyzed sample as a function of temperature (Fig. 18). A thermogravimetric analyzer is often combined with a mass spectrometer. This makes it possible to determine not only the temperature at which the sample mass changes but also the molecules responsible for this mass change. An increase in the content of cobalt in Co100-MOF-74 leads to a decrease in its thermal stability in air, which can be explained by the oxidation of cobalt with molecular oxygen. In a nitrogen atmosphere, the thermal stability of MOF-74 shows no dependence on the cobalt content.

Examples of intentional generation of defects increasing the pores in MOFs to mesopores have been described.[266, 351–353] This leads to the formation of supramolecular objects in which bulkier pores make it possible to reduce kinetic hindrances owing to higher mass transfer characteristics. In addition, the pores become more accessible and capable for storage of bulky molecules, which can be used for adsorption and catalysis. Electron microscopy can be used to monitor the presence of mesopores and the quality of MOF crystals (Fig. 19).

The stability of porous periodic MOFs after removal of solvent molecules is often assessed by comparing the X-ray powder diffraction patterns of samples after heating or degassing with the theoretical X-ray powder diffraction patte rn. In addition, diffraction data are compared with

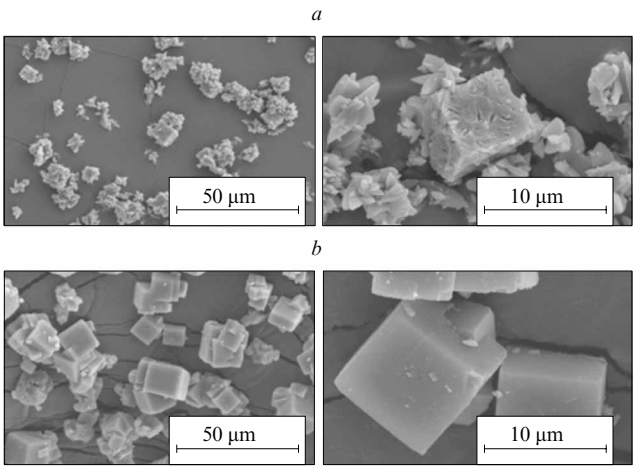

Figure 19. SEM images of S-MOF-5 prepared by the sonochemical method under different conditions: 20% power (40 W) (*a*) and 30% power (60 W) (*b*).[305]

TGA data where the stability of a structure is determined by mass changes between the desorption temperature of guest molecules and the framework disintegration temperature. Parameters of a porous framework (surface area, pore volume, size distribution of pores) are estimated by the gas adsorption isotherm method (for micro and mesopores) and mercury porometry (for macropores).[354] It should be emphasized that the use of a single method is insufficient for analysis of the MOF structure; therefore, elemental analysis (for quantification of C, N, H, metal, *etc.*), IR spectroscopy, NMR, *etc.* are used in combination with the above methods.

VIII. Analysis of MOF active sites by X-ray absorption spectroscopy

At present, X-ray absorption spectroscopy is widely used for studying the structure and properties of different catalytically active compounds, in particular, porous materials (zeolites MOFs).[44, 355, 356] Analysis of X-ray absorption near-edge structure (XANES) and extended X-ray absorption fine-structure (EXAFS) spectra considerably augments information on the local atomic and electronic structure of materials provided by other methods (electron microscopy, X-ray diffraction and optical spectroscopy).

X-Ray absorption spectroscopy methods are based on analysis of the X-ray absorption coefficient of a sample as a function of the X-ray radiation energy. Experimentally, the absorption coefficient is determined as

$$\mu(E) \sim \ln \frac{I_0}{I}$$

where I_0 and I are the intensities of the incident and transmitted radiation, respectively. Scanning in a wide energy range reveals that the absorption coefficient rapidly decreases with increasing radiation energy, but there are sharp rises in absorption against the smooth background. Such a rise in absorption, referred to as absorption edge, appears when the incident X-ray energy becomes equal to the binding energy of a core-level electron of one of the chemical elements constituting the sample. In this case, the photon energy become sufficient for excitation of electrons from this level to vacant states above the Fermi level. The core-level energies are different for different elements, and each absorption edge is generated by a definite electronic transition. In particular, the absorption edge at ~8979 eV corresponds to the transition of a copper 1s electron to vacant states, and the absorption edge at 11 564 eV is due to the transition from the platinum $2p_{3/2}$ sublevel. According to the conventional nomenclature, the transition from the 1s level is referred to as K-edge and that from the $2p_{3/2}$ level, L_3-edge of an element. It is precisely these edges that are measured in the X-ray absorption spectroscopy experiments. Table 4 lists the K- and L_3-edge energies of chemical elements.

An absorption edge always has a fine structure. In particular, there are absorption coefficient oscillations against the background, and these oscillations are discernible up to 1500 eV beyond the edge. The oscillation structure beyond each edge is determined by the density distribution of electronic states localized on the absorbing atom, as well as by the scattering of the emergent photoelectron wave on the its nearest neighbouring atoms. As mentioned above, the X-ray absorption spectrum is typically divided into two portions: the near-edge region (XANES), from a few electron-volts before the edge to several tens of electron-volts beyond the edge, and the extended fine structure region (EXAFS), which continues until oscillations finally cease. XANES spectra are sensitive to the oxidation state of the absorbing atom, bond angles and bond lengths, whereas Fourier analysis of EXAFS spectra is used to determine interatomic distances and coordination numbers.

Table 4. K- and L_3-edge energies (in eV) of chemical elements.

Edge	C	Ni	Cu	Zn	Zr	Pt
K	284	8333	8979	9659	17998	78395
L_3	7.2	853	933	1022	2223	11564

It should be emphasized that the selectivity of the XANES and EXAFS methods caused by a significant difference in absorption edge energies of different elements makes it possible to study the local environment of a definite element rather than the structure as a whole. An important consequence of the local character of X-ray absorption spectroscopy is that the presence of long-range order of the atoms of elements to be studied is not necessary, which is essential for MOFs. Indeed, whereas the framework itself exhibits periodicity and gives rise to clearly pronounced diffraction peaks, different atoms (molecules) connected to linkers have no long-range order, but are of crucial interest to catalysis since act as active sites for numerous reactions. An example of using X-ray absorption spectroscopy for identification of structures coordinated to a linker has been reported by Long and Yaghi's groups for MOF-253, the first MOF with free nitrogen donor atoms of the 2,2′-bipyridine-5,5′-dicarboxylate linker.[357] The presence of the free coordination site made it possible to functionalize the material with palladium chloride. Analysis of the Pd K-edge EXAFS spectrum of the functionalized material confirmed that the Pd atom is surrounded by two chlorine and two nitrogen atoms, the bond lengths being similar to those in (BPY)$PdCl_2$. Thus, it has been proved that palladium is actually coordinated to the bipyridine from the MOF. Analogously, but from analysis of the Pt L_3-edge EXAFS, proof has been obtained that platinum ions are coordinated to the same MOF.[358]

XANES spectra can provide information necessary for the identification of embedded species and determination of their charge state. The Pt L_3-edge XANES spectra of platinum-functionalized MOF UiO-67, separate linkers and platinum salts serving as references has been reported.[319] Compounds containing platinum(II) and platinum(IV) have been considered. After the bipyridine moieties of the MOF were doped with platinum in the form $PtCl_2$ (UiO-67-Pt^{II}) or $PtCl_4$ (UiO-67-Pt^{IV}), platinum in some samples was additionally functionalized with toluene-3,4-dithiol (TDT) molecules or bromide ions (a Br_2 solution in 2-propanol or octane) (Fig. 20 *a*). It was demonstrated that the main maximum intensity of the XANES spectrum correlates well with the coordination number of platinum determined from EXAFS. This is explained by the fact that the oxidation state of platinum atoms depends on the number of their coordinated atoms: the larger the coordination number, the higher the oxidation state. Since platinum has almost completely filled 5d shell, the increase in the

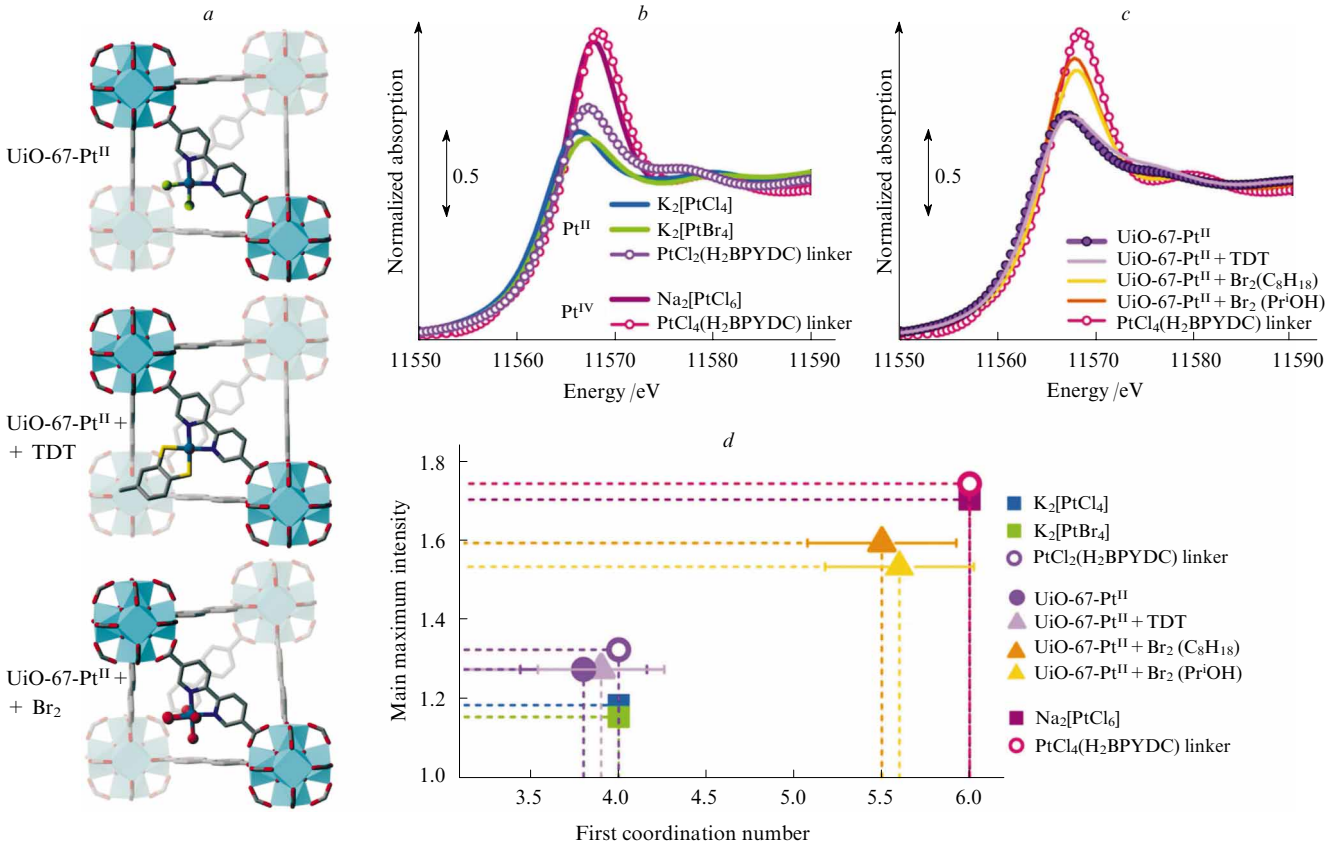

Figure 20. Schematic image of the functionalized linker 2,2′-bipyridine-5,5′-dicarboxylate (H_2BPYDC) in the structure of the initial UiO-67-Pt^{II} after the reaction with toluene-3,4-dithiol and bromine in octane or 2-propanol (*a*); Pt L_3-edge XANES spectra of compounds with the known platinum oxidation state (salts and linkers) (*b*); the same spectra for the functionalized MOFs shown in Fig. *a*; for comparison, the spectrum of the linker with tetravalent platinum is given (*c*); correlation between the main maximum intensity in the XANES spectrum and the number of atoms in the first coordination sphere of the Pt atom (*d*).[319]

oxidation state entails the increase in the number of free d-states; according to the dipole selection rules, these states accept an electron excited from the $2p_{3/2}$ sublevel when an L_3-edge spectrum is measured. Thus, there is a correlation between the coordination number of the metal atom and the main maximum intensity of the XANES.

Figure 20 *b*,*c* shows that, by the main maximum intensity of XANES, different platinum compounds are separated into two well-pronounced groups corresponding to the Pt^{II} and Pt^{IV} oxidation states. According to XANES data, the reaction of platinum sites of UiO-67 with toluene-dithiol, *i.e.*, the substitution of two sulfur atoms for two chlorine atoms, is not accompanied by a change in the platinum oxidation state, which is supported by EXAFS data demonstrating that the four-coordinate platinum sites persist (see Fig. 20 *d*). At the same time, in the reaction with bromine, whatever the solvent used, platinum is oxidized to Pt^{IV} (the main maximum of XANES increases), which is confirmed by the increase in coordination number to nearly 6, according to the EXAFS data. In this case, it can be stated that two chlorine atoms in the nearest environment of platinum are completely replaced by four bromine atoms.

In a similar way X-ray absorption spectroscopy is used for studying the character of adsorption of different molecules on the MOF metal sites. In particular, the interaction of HKUST-1 with ammonia has been considered (Fig. 21).[359] From analysis of the Cu K-edge XANES and EXAFS spectra of hydrated, dehydrated and ammonia-treated samples, the authors have determined the structural parameters of the local environment of the copper atom under these conditions and have arrived at the conclusion that ammonia chemisorption on Cu sites does not lead to the Cu–O bond cleavage but is accompanied by bond elongation, much more pronounced than in the case of coordination of a water molecule in the hydrated sample. Noteworthy is the considerable decrease of the first peak of the Fourier transform of EXAFS after the interaction of the sample with ammonia as compared with the hydrated and even dehydrated samples (see Fig. 21 *b*–*d*; upper panels). Analysis shows that this is not a result of a decrease in the number of atoms in the first coordination sphere of the copper ion, as it might seem at first glance; rather, this is caused by the fact that the scattering on the nitrogen atom is in antiphase to the scattering on the oxygen atoms (see Fig. 21 *b*–*d*; lower panels). Thus, the contributions of these atoms attenuate each other, thus leading to the decrease in the Fourier transform magnitude. Similar studies of absorption of gas molecules are carried out also for other types of MOFs, including studies with the use of *ab initio* calculations of spectra.[316, 360, 361]

In addition to studying coordinated species and adsorbed molecules, X-ray absorption spectroscopy can be

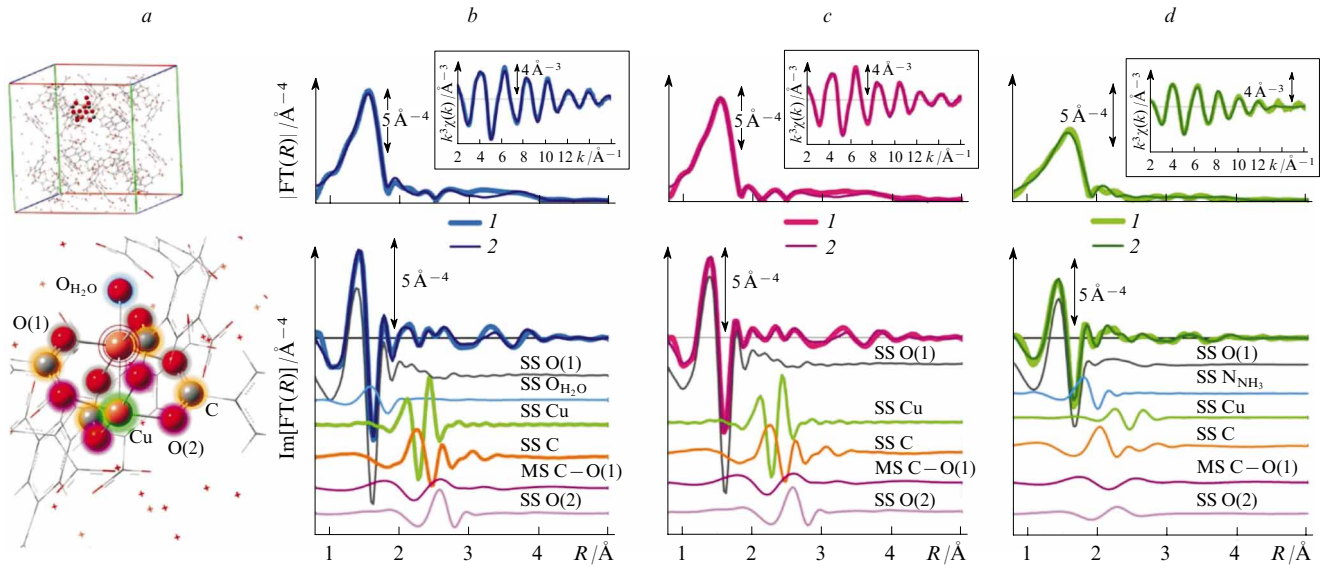

Figure 21. Structure of MOF HKUST-1 and the cluster used for optimization of structure parameters (*a*). Comparison of experimental (*1*) and theoretical (*2*) data for the hydrated sample (*b*), dehydrated sample (*c*) and the sample after the interaction with ammonia (*d*).[359] The upper panels show k^3-weighted EXAFS spectra (insets) and the corresponding Fourier transform magnitudes. The lower panels show the imaginary parts of Fourier transforms and the contributions of single scattering (SS) and multiple scattering (MS) from separate atoms.

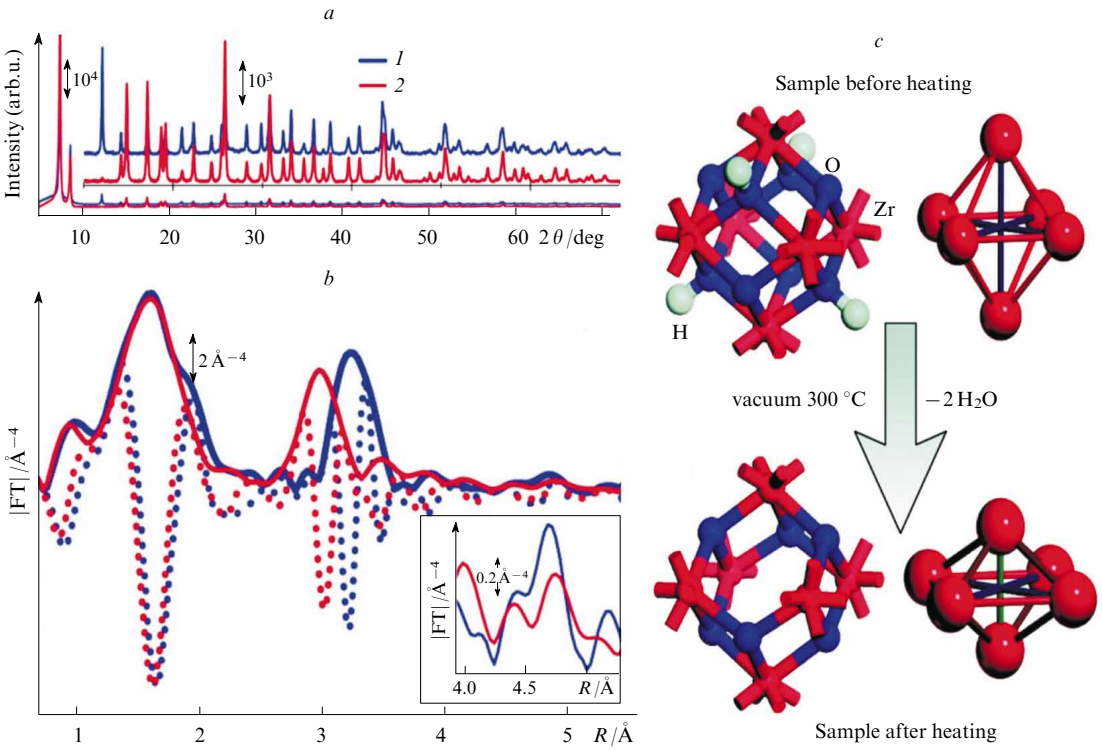

Figure 22. X-Ray powder diffraction patterns of MOF UiO-66 before and after heating and concomitant dehydration (*a*); Fourier transform magnitudes (solid curves) and imaginary parts (dotted curves) of UiO-66 before and after heating (the inset shows the region forming because of the scattering on the diagonal Zr atom) (*b*); the scheme of changes in zirconium – oxygen clusters caused by dehydration (*c*).[239]
(*a*, *b*): (*1*) The sample before heating, (*2*) the sample after heating.
(*c*): At the left, all atoms of the cluster are shown; at the right, only Zr atoms are shown (to clearly show flattening caused by dehydration).

useful for an understanding of the structure of the MOF scaffold itself, although it seems that X-ray diffraction alone should be sufficient because of the periodic structure of MOFs. Study of changes in the local structure of the already mentioned MOF UiO-66 (Ref. 238) caused by heating and concomitant dehydration of the material exemplifies the expediency of using the EXAFS method. Indeed, the diffraction patterns obtained by Valenzano *et al.*[239] before and after dehydration of the MOF were very similar to each other (Fig. 22 *a*), whereas the Zr K-edge EXAFS spectra were essentially different (see Fig. 22 *b*). This result indicates that the changes in short- and long-range order of the atoms are essentially different. In combination with quantum-chemical calculations, analysis of EXAFS data demonstrates that, in the course of dehydration, the zirconium–oxygen cluster is not only contracted losing two oxygen atoms and four hydrogen atoms but is also flattened along one of the axes (see Fig. 22 *c*). The contraction leads to the decrease in Zr–Zr distances and, respectively, to the shift of the second peak in the Fourier transform of EXAFS from 3.17 to 2.91 Å (without applying phase corrections), and the flattening leads to the decrease in the degree of degeneracy of Zr–Zr distances. The latter accounts for the appearance of a shoulder at 3.41 Å, and the weak contribution of the scattering on the Zr atom located at the opposite end of the octahedron axis (peaks in the range 4.7 Å) is almost completely diffused. Nevertheless, these significant changes are not reflected in the X-ray diffraction pattern since the flattening of zirconium octahedra occurs randomly along one of the three axes.

An additional advantage of X-ray absorption spectroscopy is the high penetration ability of X-rays, which makes it possible to carry out *in situ* spectroscopic studies using intense sources of X-rays (synchrotrons), *i.e.*, in the course of chemical reactions. This allows real-time monitoring of the changes that occur in the local atomic and electronic structure of a material. In particular, de Combarieu *et al.*[362] have studied the changes induced in the local atomic and electronic structure of iron atoms in MOF MIL-53 by electrochemical lithium insertion. The shift of the Fe K-edge toward lower energies during lithium insertion is evidence that about one-half of iron atoms, initially existing in the oxidation state Fe^{III}, is reduced to Fe^{II}. EXAFS analysis shows that the process is accompanied by an increase in Fe–O distances. It is of interest that changes in the structure and electronic properties are completely reversible; *i.e.*, after lithium extraction, the parameters return to their initial values.

* * *

MOFs constitute a relatively new but extremely actively studied class of compounds. Each year, the number of new representatives of MOFs increases, new areas of application of these materials appear, and a whole spectrum of possibilities of modern science is used for their synthesis and analysis. Such a close attention is caused by a wide range of possibilities to predict the properties of synthesized materials and a striking diversity of their structures, which can serve to synthesize materials with tailored properties. All the above makes MOFs candidate materials with promising properties, which have found application in different fields, but are still in need of further study.

This work was supported through Megagrant 14.Y26.31.0001 from the Government of the Russian Federation for State Support of Scientific Research conducted under the guidance of leading scientists. A A Guda and K A Lomachenko acknowledge support through Grant MK-3206.2014.2 from the President of the Russian Federation for Support of Young Scientists. M A Soldatov is grateful for scholarship SP-2373.2013.5 of the President of the Russian Federation for young scientists.

References

1. G T Kokotailo, S L Lawton, D H Olson, W M Meier *Nature (London)* **272** 437 (1978)
2. M E Davis, R F Lobo *Chem. Mater.* **4** 756 (1992)
3. M W Anderson, O Terasaki, T Ohsuna, A Philippou, S P Mackay, A Ferreira, J Rocha, S Lidin *Nature (London)* **367** 347 (1994)
4. B Notari *Adv. Catal.* **41** 253 (1996)
5. J Rocha, M W Anderson *Eur. J. Inorg. Chem.* 801 (2000)
6. R E Morris, X Bu *Nat. Chem.* **2** 353 (2010)
7. L Nemeth, S R Bare *Adv. Catal.* **57** 1 (2014)
8. J C Groen, L A A Peffer, J Pérez-Ramírez *Microporous Mesoporous Mater.* **60** 1 (2003)
9. A Zecchina, S Bordiga, J G Vitillo, G Ricchiardi, C Lamberti, G Spoto, M Bjørgen, K P Lillerud *J. Am. Chem. Soc.* **127** 6361 (2005)
10. R Krishna, B Smit, S Calero *Chem. Soc. Rev.* **31** 185 (2002)
11. A C McKinlay, B Xiao, D S Wragg, P S Wheatley, I L Megson, R E Morris *J. Am. Chem. Soc.* **130** 10440 (2008)
12. A Corma *J. Catal.* **216** 298 (2003)
13. A Corma *Chem. Rev.* **95** 559 (1995)
14. M Shelef *Chem. Rev.* **95** 209 (1995)
15. J F Haw, W Song, D M Marcus, J B Nicholas *Acc. Chem. Res.* **36** 317 (2003)
16. J Pérez-Ramírez, Cl H Christensen, K Egeblad, Ch H Christensen, J C Groen *Chem. Soc. Rev.* **37** 2530 (2008)
17. F X Llabrés i Xamena, P Calza, C Lamberti, C Prestipino, A Damin, S Bordiga, E Pelizzetti, A Zecchina *J. Am. Chem. Soc.* **125** 2264 (2003)
18. S Usseglio, P Calza, A Damin, C Minero, S Bordiga, C Lamberti, E Pelizzetti, A Zecchina *Chem. Mater.* **18** 3412 (2006)
19. G Agostini, S Usseglio, E Groppo, M J Uddin, C Prestipino, S Bordiga, A Zecchina, P L Solari, C Lamberti *Chem. Mater.* **21** 1343 (2009)
20. G A Ozin *Adv. Mater.* **4** 612 (1992)
21. C Lamberti *Microporous Mesoporous Mater.* **30** 155 (1999)
22. E Borello, C Lamberti, S Bordiga, A Zecchina, C O Areán *Appl. Phys. Lett.* **71** 2319 (1997)
23. S Bordiga, G T Palomino, A Zecchina, G Ranghino, E Giamello, C Lamberti *J. Chem. Phys.* **112** 3859 (2000)
24. M E Davis *Nature (London)* **417** 813 (2002)
25. A Stein *Adv. Mater.* **15** 763 (2003)
26. M Bjørgen, F Bonino, S Kolboe, K-P Lillerud, A Zecchina, S Bordiga *J. Am. Chem. Soc.* **125** 15863 (2003)
27. J A van Bokhoven, T-L Lee, M Drakopoulos, C Lamberti, S Thiey, J Zegenhagen *Nat. Mater.* **7** 551 (2008)
28. G Agostini, C Lamberti, L Palin, M Milanesio, N Danilina, B Xu, M Janousch, J A van Bokhoven *J. Am. Chem. Soc.* **132** 667 (2010)
29. J A van Bokhoven, C Lamberti *Coord. Chem. Rev.* **277–278** 275 (2014)
30. R A van Santen, G J Kramer *Chem. Rev.* **95** 637 (1995)
31. J Sauer, M Sierka *J. Comput. Chem.* **21** 1470 (2000)
32. P Sherwood, A H de Vries, M F Guest, G Schreckenbach, C R A Catlow, S A French, A A Sokol, S T Bromley, W Thiel, A J Turner, S Billeter, F Terstegen, S Thiel, J Kendrick, S C Rogers, J Casci, M Watson, F King, E Karlsen, M Sjøvoll, A Fahmi, A Schifer, C Lennartz *J. Mol. Struct. (THEOCHEM)* **632** 1 (2003)

33. A Damin, F X Llabrés i Xamena, C Lamberti, B Civalleri, C M Zicovich-Wilson, A Zecchina *J. Phys. Chem. B* **108** 1328 (2004)
34. S Bordiga, F Bonino, A Damin, C Lamberti *Phys. Chem. Chem. Phys.* **9** 4854 (2007)
35. A K Cheetham, G Fgrey, T Loiseau *Angew. Chem., Int. Ed.* **38** 3268 (1999)
36. S L James *Chem. Soc. Rev.* **32** 276 (2003)
37. D Bradshaw, J B Claridge, E J Cussen, T J Prior, M J Rosseinsky *Acc. Chem. Res.* **38** 273 (2005)
38. G Férey *Chem. Soc. Rev.* **37** 191 (2008)
39. M O'Keeffe *Chem. Soc. Rev.* **38** 1215 (2009)
40. J J Perry IV, J A Perman, M J Zaworotko *Chem. Soc. Rev.* **38** 1400 (2009)
41. H Furukawa, N Ko, Y B Go, N Aratani, S B Choi, E Choi, A Ö Yazaydin, R Q Snurr, M O'Keeffe, J Kim, O M Yaghi *Science* **329** 424 (2010)
42. O K Farha, J T Hupp *Acc. Chem. Res.* **43** 1166 (2010)
43. G Seeber, G J T Cooper, G N Newton, M H Rosnes, D-L Long, B M Kariuki, P Kögerler, L Cronin *Chem. Sci.* **1** 62 (2010)
44. S Bordiga, F Bonino, K P Lillerud, C Lamberti *Chem. Soc. Rev.* **39** 4885 (2010)
45. H-C Zhou, J R Long, O M Yaghi *Chem. Rev.* **112** 673 (2012)
46. H Furukawa, K E Cordova, M O'Keeffe, O M Yaghi *Science* **341** Art. No. 1230444 (2013)
47. F X Llabres i Xamena, I Luz, F G Cirujano, in *Metal Organic Frameworks as Heterogeneous Catalysts* (Eds F X Llabrés i Xamena, J Gascon) (Cambridge: Royal Society of Chemistry, 2013) p. 237
48. Y J Colon, R Q Snurr *Chem. Soc. Rev.* **43** 5735 (2014)
49. A Schneemann, V Bon, I Schwedler, I Senkovska, S Kaskel, R A Fischer *Chem. Soc. Rev.* **43** 6062 (2014)
50. Q-L Zhu, Q Xu *Chem. Soc. Rev.* **43** 5468 (2014)
51. V Logvinenko, D Dybtsev, V Fedin, V Drebushchak, M Yutkin *J. Therm. Anal. Calorim.* **90** 463 (2007)
52. T Loiseau, G Fgrey *J. Fluorine Chem.* **128** 413 (2007)
53. G Férey *Chem. Mater.* **13** 3084 (2001)
54. M Eddaoudi, D B Moler, H Li, B Chen, T M Reineke, M O'Keeffe, O M Yaghi *Acc. Chem. Res.* **34** 319 (2001)
55. J R Long, O M Yaghi *Chem. Soc. Rev.* **38** 1213 (2009)
56. C Baerlocher, W M Meier, D H Olson *Atlas of Zeolite Framework Types* (Amsterdam: Elsevier, 2001)
57. H Deng, S Grunder, K E Cordova, C Valente, H Furukawa, M Hmadeh, F Gándara, A C Whalley, Z Liu, S Asahina, H Kazumori, M O'Keeffe, O Terasaki, J F Stoddart, O M Yaghi *Science* **336** 1018 (2012)
58. H Furukawa, Y B Go, N Ko, Y K Park, F J Uribe-Romo, J Kim, M O'Keeffe, O M Yaghi *Inorg. Chem.* **50** 9147 (2011)
59. P Silva, S M F Vilela, J P C Tomé, F A Almeida Paz *Chem. Soc. Rev.* **44** 6774 (2015)
60. A Czaja, T Trukhan, U Müller *Chem. Soc. Rev.* **38** 1284 (2009)
61. J-R Li, R J Luppler, H-C Zhou *Chem. Soc. Rev.* **38** 1477 (2009)
62. S Qiu, G Zhu *Coord. Chem. Rev.* **253** 2891 (2009)
63. S Shimomura, M Higuchi, R Matsuda, K Yoneda, Y Hijikata, Y Kubota, Y Mita, J Kim, M Takata, S Kitagawa *Nat. Chem.* **2** 633 (2010)
64. J-R Li, J Sculley, H-C Zhou *Chem. Rev.* **112** 869 (2012)
65. S Qiu, M Xue, G Zhu *Chem. Soc. Rev.* **43** 6116 (2014)
66. M Dincă, J R Long *J. Am. Chem. Soc.* **127** 9376 (2005)
67. J G Vitillo, M Savonnet, G Ricchiardi, S Bordiga *ChemSusChem* **4** 1281 (2011)
68. S Chaemchuen, N A Kabir, K Zhou, F Verpoort *Chem. Soc. Rev.* **42** 9304 (2013)
69. C P Cabello, G Berlier, G Magnacca, P Rumori, G T Palomino *CrystEngComm* **17** 430 (2015)
70. T Rodenas, I Luz, G Prieto, B Seoane, H Miro, A Corma, F Kapteijn, F X Llabrés i Xamena, J Gascon *Nat. Mater.* **14** 48 (2015)
71. D Britt, H Furukawa, B Wang, T G Glover, O M Yaghi *Proc. Natl. Acad. Sci. USA* **106** 20637 (2009)
72. S Keskin, T M van Heest, D S Sholl *ChemSusChem* **3** 879 (2010)
73. G Férey, C Serre, T Devic, G Maurin, H Jobic, P L Llewellyn, G De Weireld, A Vimont, M Daturi, J-S Chang *Chem. Soc. Rev.* **40** 550 (2011)
74. L Pan, D H Olson, L R Ciemnolonski, R Heddy, J Li *Angew. Chem., Int. Ed.* **45** 616 (2006)
75. R Matsuda, T Tsujino, H Sato, Y Kubota, K Morishige, M Takata, S Kitagawa *Chem. Sci.* **1** 315 (2010)
76. E Barea, C Montoro, J A R Navarro *Chem. Soc. Rev.* **43** 5419 (2014)
77. J B DeCoste, G W Peterson *Chem. Rev.* **114** 5695 (2014)
78. K Suh, M P Yutkin, D N Dybtsev, V P Fedin, K Kim *Chem. Commun.* **48** 513 (2012)
79. S A Sapchenko, D G Samsonenko, D N Dybtsev, V P Fedin *Inorg. Chem.* **52** 9702 (2013)
80. Z-Y Gu, C-X Yang, N Chang, X-P Yan *Acc. Chem. Res.* **45** 734 (2012)
81. K A Cychosz, R Ahmad, A J Matzger *Chem. Sci.* **1** 293 (2010)
82. M R Kishan, J Tian, P K Thallapally, C A Fernandez, S J Dalgarno, J E Warren, B P McGrail, J L Atwood *Chem. Commun.* **46** 538 (2010)
83. Y-S Li, F-Y Liang, H Bux, A Feldhoff, W-S Yang, J Caro *Angew. Chem., Int. Ed.* **49** 548 (2010)
84. J An, S J Geib, N L Rosi *J. Am. Chem. Soc.* **132** 38 (2010)
85. A L Nuzhdin, K A Kovalenko, D N Dybtsev, G A Bukhtiyarova *Mendeleev Commun.* **20** 57 (2010)
86. B Van de Voorde, B Bueken, J Denayer, D De Vos *Chem. Soc. Rev.* **43** 5766 (2014)
87. M Kondo, T Yoshitomi, K Seki, H Matsuzaka, S Kitagawa, K Seki *Angew. Chem., Int. Ed. Engl.* **36** 1725 (1997)
88. K Sumida, S Horike, S S Kaye, Z R Herm, W L Queen, C M Brown, F Grandjean, G J Long, A Dailly, J R Long *Chem. Sci.* **1** 184 (2010)
89. R B Getman, Y-S Bae, C E Wilmer, R Q Snurr *Chem. Rev.* **112** 703 (2012)
90. H Wu, Q Gong, D H Olson, J Li *Chem. Rev.* **112** 836 (2012)
91. A Uzun, S Keskin *Prog. Surf. Sci.* **89** 56 (2014)
92. D Sun, S Ma, Y Ke, D J Collins, H-C Zhou *J. Am. Chem. Soc.* **128** 3896 (2006)
93. Y Li, R T Yang *J. Am. Chem. Soc.* **128** 726 (2006)
94. M Dincă, A Dailly, Y Liu, C M Brown, D A Neumann, J R Long *J. Am. Chem. Soc.* **128** 16876 (2006)
95. P M Forster, J Eckert, B D Heiken, J B Parise, J W Yoon, S H Jhung, J-S Chang, A K Cheetham *J. Am. Chem. Soc.* **128** 16846 (2006)
96. J G Vitillo, L Regli, S Chavan, G Ricchiardi, G Spoto, P D C Dietzel, S Bordiga, A Zecchina *J. Am. Chem. Soc.* **130** 8386 (2008)
97. L J Murray, M Dincă, J R Long *Chem. Soc. Rev.* **38** 1294 (2009)
98. S S Han, J L Mendoza-Cortés, W A Goddard III *Chem. Soc. Rev.* **38** 1460 (2009)
99. Y H Hu, L Zhang *Adv. Mater.* **22** E117 (2010)
100. D Dybtsev, C Serre, B Schmitz, B Panella, M Hirscher, M Latroche, P L Llewellyn, S Cordier, Y Molard, M Haouas, F Taulelle, G Férey *Langmuir* **26** 11283 (2010)
101. S N Klyamkin, E A Berdonosova, E V Kogan, K A Kovalenko, D N Dybtsev, V P Fedin *Chem. – Asian J.* **6** 1854 (2011)
102. K Sumida, C M Brown, Z R Herm, S Chavan, S Bordiga, J R Long *Chem. Commun.* **47** 1157 (2011)

103. S Chavan, J G Vitillo, D Gianolio, O Zavorotynska, B Civalleri, S Jakobsen, M H Nilsen, L Valenzano, C Lamberti, K P Lillerud, S Bordiga *Phys. Chem. Chem. Phys.* **14** 1614 (2012)
104. M P Suh, H J Park, T K Prasad, D-W Lim *Chem. Rev.* **112** 782 (2012)
105. M Eddaoudi, J Kim, N Rosi, D Vodak, J Wachter, M O'Keeffe, O M Yaghi *Science* **295** 469 (2002)
106. S Ma, D Sun, J M Simmons, C D Collier, D Yuan, H-C Zhou *J. Am. Chem. Soc.* **130** 1012 (2008)
107. E A Berdonosova, N V Maletskaya, E V Kogan, K A Kovalenko, S N Klyamkin, D N Dybtsev, V P Fedin *Russ. Chem. Bull., Int. Ed.* **62** 157 (2013) [*Izv. Akad. Nauk, Ser. Khim.* 159 (2013)]
108. A R Millward, O M Yaghi *J. Am. Chem. Soc.* **127** 17998 (2005)
109. P D C Dietzel, R E Johnsen, H Fjellvag, S Bordiga, E Groppo, S Chavan, R Blom *Chem. Commun.* 5125 (2008)
110. D M D'Alessandro, B Smit, J R Long *Angew. Chem., Int. Ed.* **49** 6058 (2010)
111. K Sumida, D L Rogow, J A Mason, T M McDonald, E D Bloch, Z R Herm, T-H Bae, J R Long *Chem. Rev.* **112** 724 (2012)
112. D Tanaka, A Henke, K Albrecht, M Moeller, K Nakagawa, S Kitagawa, J Groll *Nat. Chem.* **2** 410 (2010)
113. J Ethiraj, F Bonino, C Lamberti, S Bordiga *Microporous Mesoporous Mater.* **207** 90 (2015)
114. S Chavan, F Bonino, L Valenzano, B Civalleri, C Lamberti, N Acerbi, J H Cavka, M Leistner, S Bordiga *J. Phys. Chem. C* **117** 15615 (2013)
115. J Canivet, A Fateeva, Y Guo, B Coasne, D Farrusseng *Chem. Soc. Rev.* **43** 5594 (2014)
116. B Xiao, P S Wheatley, X Zhao, A J Fletcher, S Fox, A G Rossi, I L Megson, S Bordiga, L Regli, K M Thomas, R E Morris *J. Am. Chem. Soc.* **129** 1203 (2007)
117. P Horcajada, T Chalati, C Serre, B Gillet, C Sebrie, T Baati, J F Eubank, D Heurtaux, P Clayette, C Kreuz, J-S Chang, Y K Hwang, V Marsaud, P-N Bories, L Cynober, S Gil, G Férey, P Couvreur, R Gref *Nat. Mater.* **9** 172 (2010)
118. P Horcajada, R Gref, T Baati, P K Allan, G Maurin, P Couvreur, G Férey, R E Morris, C Serre *Chem. Rev.* **112** 1232 (2012)
119. E D Bloch, W L Queen, S Chavan, P S Wheatley, J M Zadrozny, R Morris, C M Brown, C Lamberti, S Bordiga, J R Long *J. Am. Chem. Soc.* **137** 3466 (2015)
120. J-C G Bünzli, C Piguet *Chem. Rev.* **102** 1897 (2002)
121. C Serre, F Millange, C Thouvenot, N Gardant, F Pelle, G Férey *J. Mater. Chem.* **14** 1540 (2004)
122. D Imbert, S Comby, A-S Chauvin, J-C G Bünzli *Chem. Commun.* 1432 (2005)
123. S Bordiga, C Lamberti, G Ricchiardi, L Regli, F Bonino, A Damin, K-P Lillerud, M Bjørgen, A Zecchina *Chem. Commun.* 2300 (2004)
124. M D Allendorf, C A Bauer, R K Bhakta, R J T Houk *Chem. Soc. Rev.* **38** 1330 (2009)
125. K A Kovalenko, D N Dybtsev, S F Lebedkin, V P Fedin *Russ. Chem. Bull., Int. Ed.* **59** 741 (2010) [*Izv. Akad. Nauk, Ser. Khim.* 727 (2010)]
126. S A Sapchenko, D N Dybtsev, D G Samsonenko, V P Fedin *New J. Chem.* **34** 2445 (2010)
127. S A Sapchenko, D G Samsonenko, D N Dybtsev, M S Melgunov, V P Fedin *Dalton Trans.* **40** 2196 (2011)
128. J-L Wang, C Wang, W Lin *ACS Catal.* **2** 2630 (2012)
129. Y Cui, Y Yue, G Qian, B Chen *Chem. Rev.* **112** 1126 (2012)
130. J Heine, K Müller-Buschbaum *Chem. Soc. Rev.* **42** 9232 (2013)
131. Y Cui, B Chen, G Qian *Coord. Chem. Rev.* **273 – 274** 76 (2014)
132. Z Hu, B J Deibert, J Li *Chem. Soc. Rev.* **43** 5815 (2014)
133. H Sato, R Matsuda, K Sugimoto, M Takata, S Kitagawa *Nat. Mater.* **9** 661 (2010)
134. D Maspoch, D Ruiz-Molina, K Wurst, N Domingo, M Cavallini, F Biscarini, J Tejada, C Rovira, J Veciana *Nat. Mater.* **2** 190 (2003)
135. D Maspoch, N Domingo, D Ruiz-Molina, K Wurst, J-M Hernández, G Vaughan, C Rovira, F Lloret, J Tejada, J Veciana *Chem. Commun.* 5035 (2005)
136. M Kurmoo *Chem. Soc. Rev.* **38** 1353 (2009)
137. M P Yutkin, M S Zavakhina, A V Virovets, D N Dybtsev, V P Fedin, T Kusamoto, H Nishihara *Inorg. Chim. Acta* **365** 513 (2011)
138. W Zhang, R-G Xiong *Chem. Rev.* **112** 1163 (2012)
139. G Férey, F Millange, M Morcrette, C Serre, M-L Doublet, J-M Grenèche, J-M Tarascon *Angew. Chem., Int. Ed.* **46** 3259 (2007)
140. S Horike, D Umeyama, S Kitagawa *Acc. Chem. Res.* **46** 2376 (2013)
141. T Yamada, K Otsubo, R Makiura, H Kitagawa *Chem. Soc. Rev.* **42** 6655 (2013)
142. V G Ponomareva, K A Kovalenko, A P Chupakhin, D N Dybtsev, E S Shutova, V P Fedin *J. Am. Chem. Soc.* **134** 15640 (2012)
143. D N Dybtsev, V G Ponomareva, S B Aliev, A P Chupakhin, M R Gallyamov, N K Moroz, B A Kolesov, K A Kovalenko, E S Shutova, V P Fedin *ACS Appl. Mater. Interfaces* **6** 5161 (2014)
144. C G Silva, A Corma, H García *J. Mater. Chem.* **20** 3141 (2010)
145. V Stavila, A A Talin, M D Allendorf *Chem. Soc. Rev.* **43** 5994 (2014)
146. Z Xie, L Ma, K E deKrafft, A Jin, W Lin *J. Am. Chem. Soc.* **132** 922 (2010)
147. P M Forster, A K Cheetham *Top. Catal.* **24** 79 (2003)
148. J Lee, O K Farha, J Roberts, K A Scheidt, S T Nguyen, J T Hupp *Chem. Soc. Rev.* **38** 1450 (2009)
149. A Corma, H García, F X Llabrés i Xamena *Chem. Rev.* **110** 4606 (2010)
150. K P Lillerud, U Olsbye, M Tilset *Top. Catal.* **53** 859 (2010)
151. M Ranocchiari, J A van Bokhoven *Phys. Chem. Chem. Phys.* **13** 6388 (2011)
152. F X Llabrés i Xamena, J Gascon, in *Metal Organic Frameworks as Heterogeneous Catalysts* (Eds F X Llabrés i Xamena, J Gascon) (Cambridge: Royal Society of Chemistry, 2013) p. 406
153. F Vermoortele, P Valvekens, D De Vos, in *Metal Organic Frameworks as Heterogeneous Catalysts* (Eds F X Llabrés i Xamena, J Gascon) (Cambridge: Royal Society of Chemistry, 2013) p. 268
154. J E Mondloch, O K Farha, J T Hupp, in *Metal Organic Frameworks as Heterogeneous Catalysts* (Eds F X Llabrés i Xamena, J Gascon) (Cambridge: Royal Society of Chemistry, 2013) p. 289
155. J Liu, L Chen, H Cui, J Zhang, L Zhang, C-Y Su *Chem. Soc. Rev.* **43** 6011 (2014)
156. B Kesanli, W Lin *Coord. Chem. Rev.* **246** 305 (2003)
157. C-D Wu, A Hu, L Zhang, W Lin *J. Am. Chem. Soc.* **127** 8940 (2005)
158. D N Dybtsev, A L Nuzhdin, H Chun, K P Bryliakov, E P Talsi, V P Fedin, K Kim *Angew. Chem., Int. Ed.* **45** 916 (2006)
159. L Ma, C Abney, W Lin *Chem. Soc. Rev.* **38** 1248 (2009)
160. D Dang, P Wu, C He, Z Xie, C Duan *J. Am. Chem. Soc.* **132** 14321 (2010)
161. Y Liu, W Xuan, Y Cui *Adv. Mater.* **22** 4112 (2010)
162. D N Dybtsev, M P Yutkin, D G Samsonenko, V P Fedin, A L Nuzhdin, A A Bezrukov, K P Bryliakov, E P Talsi, R V Belosludov, H Mizuseki, Y Kawazoe, O S Subbotin, V R Belosludov *Chem. – Eur. J.* **16** 10348 (2010)
163. G A E Oxford, D Dubbeldam, L J Broadbelt, R Q Snurr *J. Mol. Catal. A: Chem.* **334** 89 (2011)
164. M Yoon, R Srirambalaji, K Kim *Chem. Rev.* **112** 1196 (2012)

165. J M Falkowski, S Liu, W Lin, in *Metal Organic Frameworks as Heterogeneous Catalysts* (Eds F X Llabrés i Xamena, J Gascon) (Cambridge: Royal Society of Chemistry, 2013) p. 344
166. K Leus, Y-Y Liu, P Van Der Voort *Catal. Rev. Sci. Eng.* **56** 1 (2014)
167. F Song, C Wang, J M Falkowski, L Ma, W Lin *J. Am. Chem. Soc.* **132** 15390 (2010)
168. S Abednatanzi, A Abbasi, M Masteri-Farahani *J. Mol. Catal. A: Chem.* **399** 10 (2015)
169. D Jiang, A Urakawa, M Yulikov, T Mallat, G Jeschke, A Baiker *Chem. – Eur. J.* **15** 12255 (2009)
170. K Schlichte, T Kratzke, S Kaskel *Microporous Mesoporous Mater.* **73** 81 (2004)
171. F X Llabrés i Xamena, A Abad, A Corma, H Garcia *J. Catal.* **250** 294 (2007)
172. B Xiao, H Hou, Y Fan *J. Organomet. Chem.* **692** 2014 (2007)
173. S Proch, J Herrmannsdörfer, R Kempe, C Kern, A Jess, L Seyfarth, J Senker *Chem. – Eur. J.* **14** 8204 (2008)
174. H Liu, Y Liu, Y Li, Z Tang, H Jiang *J. Phys. Chem. C* **114** 13362 (2010)
175. D Jiang, T Mallat, D M Meier, A Urakawa, A Baiker *J. Catal.* **270** 26 (2010)
176. S Gao, N Zhao, M Shu, S Che *Appl. Catal., A: Gen.* **388** 196 (2010)
177. M Annapurna, T Parsharamulu, P V Reddy, M Suresh, P R Likhar, M L Kantam *Appl. Organomet. Chem.* **29** 234 (2015)
178. F Vermoortele, R Ameloot, A Vimont, C Serre, D De Vos *Chem. Commun.* **47** 1521 (2011)
179. J Gascon, U Aktay, M D Hernandez-Alonso, G P M van Klink, F Kapteijn *J. Catal.* **261** 75 (2009)
180. J Juan-Alcañiz, E V Ramos-Fernandez, U Lafont, J Gascon, F Kapteijn *J. Catal.* **269** 229 (2010)
181. J Juan-Alcañiz, E V Ramos-Fernandez, F Kapteijn, J Gascon, in *Metal Organic Frameworks as Heterogeneous Catalysts* (Eds F X Llabrés i Xamena, J Gascon) (Cambridge: Royal Society of Chemistry, 2013) p. 310
182. Y Goto, H Sato, S Shinkai, K Sada *J. Am. Chem. Soc.* **130** 14354 (2008)
183. I Luz, F X Llabrés i Xamena, A Corma *J. Catal.* **276** 134 (2010)
184. S Horike, M Dincă, K Tamaki, J R Long *J. Am. Chem. Soc.* **130** 5854 (2008)
185. M Savonnet, S Aguado, U Ravon, D Bazer-Bachi, V Lecocq, N Bats, C Pinel, D Farrusseng *Green Chem.* **11** 1729 (2009)
186. A M Shultz, O K Farha, J T Hupp, S T Nguyen *J. Am. Chem. Soc.* **131** 4204 (2009)
187. J Song, Z Zhang, S Hu, T Wu, T Jiang, B Han *Green Chem.* **11** 1031 (2009)
188. A Dhakshinamoorthy, M Alvaro, H García *Adv. Synth. Catal.* **352** 3022 (2010)
189. C G Silva, I Luz, F X Llabres i Xamena, A Corma, H García *Chem. – Eur. J.* **16** 11133 (2010)
190. H García, B Ferrer, in *Metal Organic Frameworks as Heterogeneous Catalysts* (Eds F X Llabrés i Xamena, J Gascon) (Cambridge: Royal Society of Chemistry, 2013) p. 365
191. S Lim, K Suh, Y Kim, M Yoon, H Park, D N Dybtsev, K Kim *Chem. Commun.* **48** 7447 (2012)
192. S P Gabuda, S G Kozlova, D N Dybtsev, V P Fedin *J. Struct. Chem.* **50** 887 (2009) [*Zh. Strukt. Khim.* **50** 924 (2009)]
193. S P Gabuda, S G Kozlova, D G Samsonenko, D N Dybtsev, V P Fedin *J. Phys. Chem. C* **115** 20460 (2011)
194. O M Yaghi, G Li, H Li *Nature (London)* **378** 703 (1995)
195. H Li, M Eddaoudi, T L Groy, O M Yaghi *J. Am. Chem. Soc.* **120** 8571 (1998)
196. H Li, M Eddaoudi, M O'Keeffe, O M Yaghi *Nature (London)* **402** 276 (1999)
197. S Kaskel, F Schüth, M Stöcker *Microporous Mesoporous Mater.* **73** 1 (2004)
198. K Maeda *Microporous Mesoporous Mater.* **73** 47 (2004)
199. W Mori, S Takamizawa, C N Kato, T Ohmura, T Sato *Microporous Mesoporous Mater.* **73** 31 (2004)
200. M J Rosseinsky *Microporous Mesoporous Mater.* **73** 15 (2004)
201. J L C Rowsell, O M Yaghi *Microporous Mesoporous Mater.* **73** 3 (2004)
202. P M Forster, A K Cheetham *Microporous Mesoporous Mater.* **73** 57 (2004)
203. H Hanika-Heidl, R D Fischer *Microporous Mesoporous Mater.* **73** 65 (2004)
204. C I Ratcliffe, D V Soldatov, J A Ripmeester *Microporous Mesoporous Mater.* **73** 71 (2004)
205. H-L Sun, S Gao, B-Q Ma, F Chang, W-F Fu *Microporous Mesoporous Mater.* **73** 89 (2004)
206. S-Y Wan, Y-T Huang, Y-Z Li, W-Y Sun *Microporous Mesoporous Mater.* **73** 101 (2004)
207. Q Wei, M Nieuwenhuyzen, S L James *Microporous Mesoporous Mater.* **73** 97 (2004)
208. S T Meek, J A Greathouse, M D Allendorf *Adv. Mater.* **23** 141 (2011)
209. B Panella, M Hirscher, in *Encyclopedia of Electrochemical Power Sources* (Ed. J Garche) (Amsterdam: Elsevier, 2009) p. 493
210. S Calero, in *Comprehensive Inorganic Chemistry II* Vol. 9 (2nd Ed.) (Eds J Reedijk, K Poeppelmeier) (Amsterdam; Elsevier, 2013) p. 989
211. Y-R Lee, J Kim, W-S Ahn *Korean J. Chem. Eng.* **30** 1667 (2013)
212. O Shekhah, J Liu, R A Fischer, C Wlll *Chem. Soc. Rev.* **40** 1081 (2011)
213. M P Yutkin, D N Dybtsev, V P Fedin *Russ. Chem. Rev.* **80** 1009 (2011)
214. P Valvekens, F Vermoortele, D De Vos *Catal. Sci. Technol.* **3** 1435 (2013)
215. S M Cohen *Chem. Rev.* **112** 970 (2012)
216. N Stock, S Biswas *Chem. Rev.* **112** 933 (2012)
217. P Horcajada, C Serre, R Gref, P Couvreur, in *Comprehensive Biomaterials* (Ed. P Ducheyne) (Oxford: Elsevier, 2011) p. 559
218. A Bétard, R A Fischer *Chem. Rev.* **112** 1055 (2012)
219. Q Fang, J Sculley, H-C J Zhou, G Zhu, in *Comprehensive Nanoscience and Technology* Vol. 5 (Eds D L Andrews, G D Scholes, G P Wiederrecht) (Amsterdam: Academic Press, 2011) p. 1
220. *Metal Organic Frameworks as Heterogeneous Catalysts* (Eds F X Llabrés i Xamena, J Gascon) (Cambridge: Royal Society of Chemistry, 2013)
221. *Metal-Organic Frameworks: Applications from Catalysis to Gas Storage* (Ed. D Farrusseng) (Wiley-VCH, 2011)
222. *Metal-Organic Frameworks: Design, Application* (Ed. L R MacGillivray) (Hoboken, NJ: Wiley, 2010)
223. B Moulton, M J Zaworotko *Curr. Opin. Solid State Mater. Sci.* **6** 117 (2002)
224. S V Vinogradova, O V Vinogradova *Russ. Chem. Rev.* **44** 510 (1975)
225. S Subramanian, M J Zaworotko *Angew. Chem., Int. Ed. Engl.* **34** 2127 (1995)
226. W Siebert *Russ. Chem. Rev.* **60** 784 (1991)
227. P J Hagrman, D Hagrman, J Zubieta *Angew. Chem., Int. Ed.* **38** 2638 (1999)
228. Y Aoyama *Top. Curr. Chem.* **198** 131 (1998)
229. C Janiak *Dalton Trans.* 2781 (2003)
230. O M Yaghi, M O'Keeffe, N W Ockwig, H K Chae, M Eddaoudi, J Kim *Nature (London)* **423** 705 (2003)
231. M P Yutkin, M S Zavakhina, D G Samsonenko, D N Dybtsev, V P Fedin *Russ. Chem. Bull., Int. Ed.* **59** 733 (2010) [*Izv. Akad. Nauk, Ser. Khim.* 719 (2010)]

232. M P Yutkin, M S Zavakhina, D G Samsonenko, D N Dybtsev, V P Fedin *Inorg. Chim. Acta* **394** 367 (2013)
233. M S Zavakhina, D G Samsonenko, A V Virovets, D N Dybtsev, V P Fedin *J. Solid State Chem.* **210** 125 (2014)
234. M S Zavakhina, M P Yutkin, D G Samsonenko, D N Dybtsev, V P Fedin *Russ. Chem. Bull., Int. Ed.* **60** 2425 (2011) [*Izv. Akad. Nauk, Ser. Khim.* 2378 (2011)]
235. J-S Hu, Z Lei, C-L Pan, J He *Mendeleev Commun.* **24** 290 (2014)
236. J-S Hu, X-M Zhang, H-L Xing, J He, J-J Shi *Mendeleev Commun.* **23** 231 (2013)
237. D J Tranchemontagne, J L Mendoza-Cortés, M O'Keeffe, O M Yaghi *Chem. Soc. Rev.* **38** 1257 (2009)
238. J H Cavka, S Jakobsen, U Olsbye, N Guillou, C Lamberti, S Bordiga, K P Lillerud *J. Am. Chem. Soc.* **130** 13850 (2008)
239. L Valenzano, B Civalleri, S Chavan, S Bordiga, M H Nilsen, S Jakobsen, K P Lillerud, C Lamberti *Chem. Mater.* **23** 1700 (2011)
240. M Eddaoudi, J Kim, J B Wachter, H K Chae, M O'Keeffe, O M Yaghi *J. Am. Chem. Soc.* **123** 4368 (2001)
241. M Eddaoudi, J Kim, M O'Keeffe, O M Yaghi *J. Am. Chem. Soc.* **124** 376 (2002)
242. N L Rosi, M Eddaoudi, J Kim, M O'Keeffe, O M Yaghi *CrystEngComm* **4** 401 (2002)
243. S Chavan, J G Vitillo, M J Uddin, F Bonino, C Lamberti, E Groppo, K-P Lillerud, S Bordiga *Chem. Mater.* **22** 4602 (2010)
244. M Kandiah, S Usseglio, S Svelle, U Olsbye, K P Lillerud, M Tilset *J. Mater. Chem.* **20** 9848 (2010)
245. S J Garibay, S M Cohen *Chem. Commun.* **46** 7700 (2010)
246. H K Chae, D Y Siberio-Pérez, J Kim, Y Go, M Eddaoudi, A J Matzger, M O'Keeffe, O M Yaghi *Nature (London)* **427** 523 (2004)
247. E Haque, J E Lee, I T Jang, Y K Hwang, J-S Chang, J Jegal, S H Jhung *J. Hazard. Mater.* **181** 535 (2010)
248. C Chen, M Zhang, Q Guan, W Li *Chem. Eng. J.* **183** 60 (2012)
249. E Haque, J W Jun, S H Jhung *J. Hazard. Mater.* **185** 507 (2011)
250. S-H Huo, X-P Yan *J. Mater. Chem.* **22** 7449 (2012)
251. M R Ryder, J-C Tan *Mater. Sci. Technol.* **30** 1598 (2014)
252. S-L Li, Q Xu *Energy Environ. Sci.* **6** 1656 (2013)
253. C Wang, K E deKrafft, W Lin *J. Am. Chem. Soc.* **134** 7211 (2012)
254. J He, Z Yan, J Wang, J Xie, L Jiang, Y Shi, F Yuan, F Yu, Y Sun *Chem. Commun.* **49** 6761 (2013)
255. M Yoon, K Suh, S Natarajan, K Kim *Angew. Chem., Int. Ed.* **52** 2688 (2013)
256. A Morozan, F Jaouen *Energy Environ. Sci.* **5** 9269 (2012)
257. K Saravanan, M Nagarathinam, P Balaya, J J Vittal *J. Mater. Chem.* **20** 8329 (2010)
258. X Xu, R Cao, S Jeong, J Cho *Nano Lett.* **12** 4988 (2012)
259. S J Yang, S Nam, T Kim, J H Im, H Jung, J H Kang, S Wi, B Park, C R Park *J. Am. Chem. Soc.* **135** 7394 (2013)
260. W Chaikittisilp, K Ariga, Y Yamauchi *J. Mater. Chem. A* **1** 14 (2013)
261. F Meng, Z Fang, Z Li, W Xu, M Wang, Y Liu, J Zhang, W Wang, D Zhao, X Guo *J. Mater. Chem. A* **1** 7235 (2013)
262. C-K Lin, D Zhao, W-Y Gao, Z Yang, J Ye, T Xu, Q Ge, S Ma, D-J Liu *Inorg. Chem.* **51** 9039 (2012)
263. N Liedana, P Lozano, A Galve, C Tellez, J Coronas *J. Mater. Chem. B* **2** 1144 (2014)
264. N J Hinks, A C McKinlay, B Xiao, P S Wheatley, R E Morris *Microporous Mesoporous Mater.* **129** 330 (2010)
265. T Baati, L Njim, F Neffati, A Kerkeni, M Bouttemi, R Gref, M F Najjar, A Zakhama, P Couvreur, C Serre, P Horcajada *Chem. Sci.* **4** 1597 (2013)
266. G C Shearer, S Chavan, J Ethiraj, J G Vitillo, S Svelle, U Olsbye, C Lamberti, S Bordiga, K P Lillerud *Chem. Mater.* **26** 4068 (2014)
267. J Hafizovic, M Bjørgen, U Olsbye, P D C Dietzel, S Bordiga, C Prestipino, C Lamberti, K P Lillerud *J. Am. Chem. Soc.* **129** 3612 (2007)
268. E Biemmi, S Christian, N Stock, T Bein *Microporous Mesoporous Mater.* **117** 111 (2009)
269. D J Tranchemontagne, J R Hunt, O M Yaghi *Tetrahedron* **64** 8553 (2008)
270. L Huang, H Wang, J Chen, Z Wang, J Sun, D Zhao, Y Yan *Microporous Mesoporous Mater.* **58** 105 (2003)
271. K S Park, Z Ni, A P CoItg, J Y Choi, R Huang, F J Uribe-Romo, H K Chae, M O'Keeffe, O M Yaghi *Proc. Natl. Acad. Sci. USA* **103** 10186 (2006)
272. J Cravillon, S Münzer, S-J Lohmeier, A Feldhoff, K Huber, M Wiebcke *Chem. Mater.* **21** 1410 (2009)
273. X-C Huang, Y-Y Lin, J-P Zhang, X-M Chen *Angew. Chem., Int. Ed.* **45** 1557 (2006)
274. J Li, S Cheng, Q Zhao, P Long, J Dong *Int. J. Hydrogen Energy* **34** 1377 (2009)
275. S Brunauer, P H Emmett, E Teller *J. Am. Chem. Soc.* **60** 309 (1938)
276. N Simon, J Marrot, T Loiseau, G Férey *Solid State Sci.* **8** 1361 (2006)
277. T Loiseau, C Mellot-Draznieks, H Muguerra, G Férey, M Haouas, F Taulelle *C.R. Chimie* **8** 765 (2005)
278. T Loiseau, L Beitone, F Taulelle, G Férey *Solid State Sci.* **8** 346 (2006)
279. C Volkringer, T Loiseau, N Guillou, G Férey, D Popov, M Burghammer, C Riekel *Solid State Sci.* **26** 38 (2013)
280. C Volkringer, T Loiseau, N Guillou, G Férey, E Elkaïm *Solid State Sci.* **11** 1507 (2009)
281. M Riou-Cavellec, M Sanselme, J-M Grenèche, G Férey *Solid State Sci.* **2** 717 (2000)
282. M Riou-Cavellec, M Sanselme, M Noguès, J-M Grenèche, G Férey *Solid State Sci.* **4** 619 (2002)
283. M Sanselme, M Riou-Cavellec, J-M Grenèche, G Férey *J. Solid State Chem.* **164** 354 (2002)
284. M Riou-Cavellec, G Férey *Solid State Sci.* **4** 1221 (2002)
285. M Sanselme, J-M Grenèche, M Riou-Cavellec, G Férey *Solid State Sci.* **6** 853 (2004)
286. B L Hayes *Microwave Synthesis: Chemistry at the Speed of Light* (Matthews, NC: CEM Publ., 2002)
287. *Microwaves in Nanoparticle Synthesis: Fundamentals and Applications* (Eds S Horikoshi, N Serpone) (Weinheim: Wiley-VCH, 2013)
288. S H Jhung, J-H Lee, J-S Chang *Bull. Korean Chem. Soc.* **26** 880 (2005)
289. G Férey, C Serre, C Mellot-Draznieks, F Millange, S Surblé, J Dutour, I Margiolaki *Angew. Chem., Int. Ed.* **43** 6296 (2004)
290. K M L Taylor-Pashow, J D Rocca, Z Xie, S Tran, W Lin *J. Am. Chem. Soc.* **131** 14261 (2009)
291. S H Jhung, J-H Lee, J W Yoon, C Serre, G Fgrey, J-S Chang *Adv. Mater.* **19** 121 (2007)
292. N A Khan, I J Kang, H Y Seok, S H Jhung *Chem. Eng. J.* **166** 1152 (2011)
293. Y-K Seo, G Hundal, I T Jang, Y K Hwang, C-H Jun, J-S Chang *Microporous Mesoporous Mater.* **119** 331 (2009)
294. U Mueller, M Schubert, F Teich, H Puetter, K Schierle-Arndt, J Pastré *J. Mater. Chem.* **16** 626 (2006)
295. M Hartmann, S Kunz, D Himsl, O Tangermann, S Ernst, A Wagener *Langmuir* **24** 8634 (2008)

296. T R C Van Assche, G Desmet, R Ameloot, D E De Vos, H Terryn, J F M Denayer *Microporous Mesoporous Mater.* **158** 209 (2012)
297. S L James, C J Adams, C Bolm, D Braga, P Collier, T Friščić, F Grepioni, K D M Harris, G Hyett, W Jones, A Krebs, J Mack, L Maini, A G Orpen, I P Parkin, W C Shearouse, J W Steed, D C Waddell *Chem. Soc. Rev.* **41** 413 (2012)
298. V V Boldyrev *Russ. Chem. Rev.* **75** 177 (2006)
299. A Pichon, A Lazuen-Garay, S L James *CrystEngComm* **8** 211 (2006)
300. A Pichon, S L James *CrystEngComm* **10** 1839 (2008)
301. W Yuan, A L Garay, A Pichon, R Clowes, C D Wood, A I Cooper, S L James *CrystEngComm.* **12** 4063 (2010)
302. M Klimakow, P Klobes, A F Thünemann, K Rademann, F Emmerling *Chem. Mater.* **22** 5216 (2010)
303. J S Pearsall *Cavitation* (London: Mills and Boon, 1972)
304. L-G Qiu, Z-Q Li, Y Wu, W Wang, T Xu, X Jiang *Chem. Commun.* 3642 (2008)
305. W-J Son, Jun Kim, Jah Kim, W-S Ahn *Chem. Commun.* 6336 (2008)
306. Z-Q Li, L-G Qiu, T Xu, Y Wu, W Wang, Z-Y Wu, X Jiang *Mater. Lett.* **63** 78 (2009)
307. M Schlesinger, S Schulze, M Hietschold, M Mehring *Microporous Mesoporous Mater.* **132** 121 (2010)
308. Z Wang, S M Cohen *Chem. Soc. Rev.* **38** 1315 (2009)
309. H Deng, C J Doonan, H Furukawa, R B Ferreira, J Towne, C B Knobler, B Wang, O M Yaghi *Science* **327** 846 (2010)
310. B Chen, S Xiang, G Qian *Acc. Chem. Res.* **43** 1115 (2010)
311. K K Tanabe, S M Cohen *Chem. Soc. Rev.* **40** 498 (2011)
312. A D Burrows, in *Metal Organic Frameworks as Heterogeneous Catalysts* (Eds F X Llabrés i Xamena, J Gascon) (Cambridge: Royal Society of Chemistry, 2013) p. 31
313. P Deria, J E Mondloch, O Karagiaridi, W Bury, J T Hupp, O K Farha *Chem. Soc. Rev.* **43** 5896 (2014)
314. J D Evans, C J Sumby, C J Doonan *Chem. Soc. Rev.* **43** 5933 (2014)
315. W Lu, Z Wei, Z-Y Gu, T-F Liu, Jin Park, Jih Park, J Tian, M Zhang, Q Zhang, T Gentle III, M Bosch, H-C Zhou *Chem. Soc. Rev.* **43** 5561 (2014)
316. K C Szeto, K P Lillerud, M Tilset, M Bjørgen, C Prestipino, A Zecchina, C Lamberti, S Bordiga *J. Phys. Chem. B* **110** 21509 (2006)
317. K C Szeto, C Prestipino, C Lamberti, A Zecchina, S Bordiga, M Bjørgen, M Tilset, K P Lillerud *Chem. Mater.* **19** 211 (2007)
318. K C Szeto, K O Kongshaug, S Jakobsen, M Tilset, K P Lillerud *Dalton Trans.* 2054 (2008)
319. S Øien, G Agostini, S Svelle, E Borfecchia, K A Lomachenko, L Mino, E Gallo, S Bordiga, U Olsbye, K P Lillerud, C Lamberti *Chem. Mater.* **27** 1042 (2015)
320. T Kamegawa, T Sakai, M Matsuoka, M Anpo *J. Am. Chem. Soc.* **127** 16784 (2005)
321. S S Kaye, J R Long *J. Am. Chem. Soc.* **130** 806 (2008)
322. T Gadzikwa, O K Farha, C D Malliakas, M G Kanatzidis, J T Hupp, S T Nguyen *J. Am. Chem. Soc.* **131** 13613 (2009)
323. W Morris, C J Doonan, H Furukawa, R Banerjee, O M Yaghi *J. Am. Chem. Soc.* **130** 12626 (2008)
324. K K Tanabe, Z Wang, S M Cohen *J. Am. Chem. Soc.* **130** 8508 (2008)
325. C J Doonan, W Morris, H Furukawa, O M Yaghi *J. Am. Chem. Soc.* **131** 9492 (2009)
326. T Gadzikwa, O K Farha, K L Mulfort, J T Hupp, S T Nguyen *Chem. Commun.* 3720 (2009)
327. M J Ingleson, J P Barrio, J-B Guilbaud, Y Z Khimyak, M J Rosseinsky *Chem. Commun.* 2680 (2008)
328. M J Ingleson, R Heck, J A Gould, M J Rosseinsky *Inorg. Chem.* **48** 9986 (2009)
329. D-Y Hong, Y K Hwang, C Serre, G Férey, J-S Chang *Adv. Funct. Mater.* **19** 1537 (2009)
330. S Hermes, M-K Schröter, R Schmid, L Khodeir, M Muhler, A Tissler, R W Fischer, R A Fischer *Angew. Chem., Int. Ed.* **44** 6237 (2005)
331. Y Huang, Z Zheng, T Liu, J Lü, Z Lin, H Li, R Cao *Catal. Commun.* **14** 27 (2011)
332. J Juan-Alcaniz, J Gascon, F Kapteijn *J. Mater. Chem.* **22** 10102 (2012)
333. H Zhao, H Song, L Chou *Inorg. Chem. Commun.* **15** 261 (2012)
334. T Uemura, N Yanai, S Kitagawa *Chem. Soc. Rev.* **38** 1228 (2009)
335. R J T Houk, B W Jacobs, F E Gabaly, N N Chang, A A Talin, D D Graham, S D House, I M Robertson, M D Allendorf *Nano Lett.* **9** 3413 (2009)
336. K Sugikawa, Y Furukawa, K Sada *Chem. Mater.* **23** 3132 (2011)
337. G Li, H Kobayashi, J M Taylor, R Ikeda, Y Kubota, K Kato, M Takata, T Yamamoto, S Toh, S Matsumura, H Kitagawa *Nat. Mater.* **13** 802 (2014)
338. F Ke, L-G Qiu, Y-P Yuan, X Jiang, J-F Zhu *J. Mater. Chem.* **22** 9497 (2012)
339. M H Alkordi, Y Liu, R W Larsen, J F Eubank, M Eddaoudi *J. Am. Chem. Soc.* **130** 12639 (2008)
340. B Yuan, Y Pan, Y Li, B Yin, H Jiang *Angew. Chem., Int. Ed.* **49** 4054 (2010)
341. F Schröder, D Esken, M Cokoja, M W E van den Berg, O I Lebedev, G Van Tendeloo, B Walaszek, G Buntkowsky, H-H Limbach, B Chaudret, R A Fischer *J. Am. Chem. Soc.* **130** 6119 (2008)
342. M Meilikhov, K Yusenko, D Esken, S Turner, G Van Tendeloo, R A Fischer *Eur. J. Inorg. Chem.* **2010** 3701 (2010)
343. T Ishida, N Kawakita, T Akita, M Haruta *Gold Bull.* **42** 267 (2009)
344. Y E Cheon, M P Suh *Angew. Chem., Int. Ed.* **48** 2899 (2009)
345. Y K Hwang, D-Y Hong, J-S Chang, S H Jhung, Y-K Seo, J Kim, A Vimont, M Daturi, C Serre, G Férey *Angew. Chem., Int. Ed.* **47** 4144 (2008)
346. M Sabo, A Henschel, H Fröde, E Klemm, S Kaskel *J. Mater. Chem.* **17** 3827 (2007)
347. T Tsuruoka, H Kawasaki, H Nawafune, K Akamatsu *ACS Appl. Mater. Interfaces* **3** 3788 (2011)
348. J Sanchez Costa, P Gamez, C A Black, O Roubeau, S J Teat, J Reedijk *Eur. J. Inorg. Chem.* **2008** 1551 (2008)
349. A Phan, C J Doonan, F J Uribe-Romo, C B Knobler, M O'Keeffe, O M Yaghi *Acc. Chem. Res.* **43** 58 (2009)
350. J A Botas, G Calleja, M Sanchez-Sanchez, M G Orcajo *Int. J. Hydrogen Energy* **36** 10834 (2011)
351. V Guillerm, D Kim, J F Eubank, R Luebke, X Liu, K Adil, M S Lah, M Eddaoudi *Chem. Soc. Rev.* **43** 6141 (2014)
352. S Furukawa, J Reboul, S Diring, K Sumida, S Kitagawa *Chem. Soc. Rev.* **43** 5700 (2014)
353. D Bradshaw, S El-Hankari, L Lupica-Spagnolo *Chem. Soc. Rev.* **43** 5431 (2014)
354. T J Barton, L M Bull, W G Klemperer, D A Loy, B McEnaney, M Misono, P A Monson, G Pez, G W Scherer, J C Vartuli, O M Yaghi *Chem. Mater.* **11** 2633 (1999)
355. S Bordiga, E Groppo, G Agostini, J A van Bokhoven, C Lamberti *Chem. Rev.* **113** 1736 (2013)
356. E Borfecchia, D Gianolio, G Agostini, S Bordiga, C Lamberti, in *Metal Organic Frameworks as Heterogeneous Catalysts* (Eds F X Llabrés i Xamena, J Gascon) (Cambridge: Royal Society of Chemistry, 2013) p. 143
357. E D Bloch, D Britt, C Lee, C J Doonan, F J Uribe-Romo, H Furukawa, J R Long, O M Yaghi *J. Am. Chem. Soc.* **132** 14382 (2010)
358. T Zhou, Y Du, A Borgna, J Hong, Y Wang, J Han, W Zhang, R Xu *Energy Environ. Sci.* **6** 3229 (2013)

359. E Borfecchia, S Maurelli, D Gianolio, E Groppo, M Chiesa, F Bonino, C Lamberti *J. Phys. Chem. C* **116** 19839 (2012)
360. L Valenzano, J G Vitillo, S Chavan, B Civalleri, F Bonino, S Bordiga, C Lamberti *Catal. Today* **182** 67 (2012)
361. S A Guda, A A Guda, M A Soldatov, K A Lomachenko, A L Bugaev, C Lamberti, W Gawelda, C Bressler, G Smolentsev, A V Soldatov, Y Joly *J. Chem. Theory Comput.* **11** 4512 (2015)
362. G de Combarieu, S Hamelet, F Millange, M Morcrette, J-M Tarascon, G Férey, R I Walton *Electrochem. Commun.* **11** 1881 (2009)